Nuclear Physics B337 (1990) 569–634
North-Holland

SOFT AMPLITUDES IN HOT GAUGE THEORIES: A GENERAL ANALYSIS

Eric BRAATEN

Department of Physics and Astronomy, Northwestern University, Evanston, IL 60208, USA

Robert D. PISARSKI

Fermi National Accelerator Laboratory, P.O. Box 500, Batavia, IL 60510, USA
and
Department of Physics, Brookhaven National Laboratory, Upton, NY 11973, USA*

Received 10 October 1989
(Revised 1 December 1989)

A systematic method for the calculation of amplitudes in hot gauge theories is developed. It is necessary to distinguish between hard momenta (of order T) and soft momenta (of order gT). Ordinary perturbation theory applies at hard momenta, but over soft momenta, effective propagators and vertices are required. These effective quantities resum the leading contributions from thermal fluctuations with hard virtual momenta. These "hard thermal loops" arise solely from subdiagrams at one-loop order: they are ultraviolet finite, gauge independent, and satisfy simple Ward identities. To illustrate the method we apply it to the quark and gluon self-energies. Ward identities are used to show that to one-loop order in this effective perturbation expansion, the two-point $\mathscr{T}$-matrix elements constructed from the self-energies are gauge invariant. This proves that to leading order in g, the quark and gluon damping rates are gauge invariant.

1. Introduction

Gauge theories at a temperature T are of interest in a variety of problems, such as the early universe and the collisions of nuclei at ultrarelativistic energies [1]. The thermodynamic behavior near equilibrium is determined by the behavior of amplitudes obtained by the analytic continuation of euclidean Green functions from imaginary to real time. In this paper we use perturbation theory to study amplitudes in hot gauge theories; by "hot" we mean that the temperature T is much larger than any intrinsic mass scale in the problem.

Recently there has been much interest in a basic amplitude in hot QCD, the imaginary part of the gluon self-energy on mass-shell. This is a physical quantity, determining the crossover from damping by gluons to damping by hydrodynamic modes. At zero temperature general arguments show that $\mathscr{T}$-matrix elements formed by setting two-point amplitudes on mass-shell are independent of gauge,

* Present address.

0550-3213/90/$03.50

and have discontinuities of positive sign [2]. Explicit calculations at one-loop order appear to show that this property fails at nonzero temperature – both the sign and the magnitude of the gluon damping rate seem to be gauge dependent [3].

In this paper we show that these calculations are incomplete, in that they do not include all effects of leading order in the coupling constant g [4]. In hot gauge theories the usual connection between the order of the loop expansion and powers of g is lost: effects of leading order in g arise from every order in the loop expansion. We develop a systematic procedure which resums this infinite subset of graphs, implementing the program of resummation proposed by Pisarski [5]. Applying this resummation to the damping rates, we show that the resulting damping rates are gauge invariant, in accord with general expectation. A summary of the proof for the gluon damping rate appeared in ref. [6].

The need for resummation is apparent from the example of a hot scalar theory with quartic self-coupling g^2. Hot implies that the scalar is massless at tree level. The effects of nonzero temperature are familiar: the tadpole diagram generates a temperature dependent effective mass $m_s \sim gT$. Here resummation is just a matter of replacing the bare propagator, $1/P^2$, by an effective one, $1/(P^2 + m_s^2)$. For the scalar theory this is all there is to the resummation: since the running coupling constant depends upon temperature only through logarithms, and not powers of T, it suffices to use the bare vertex.

This kind of resummation is standard. The classic example is a degenerate electron gas, as treated by Gell-Mann and Brueckner [7]. It is also familiar from the study of the symmetry restoration at nonzero temperature [8]. In both of these cases, the induced mass is just a constant.

Although the principle remains the same, the resummation required in hot gauge theories is more intricate than in a scalar theory. The self-energy which enters into the effective propagator is no longer simply a mass term, but depends nontrivially on the momentum. It is also necessary to use effective vertices, with nontrivial momentum dependence, instead of bare vertices.

To explain this resummation we introduce some technical concepts. Real-time amplitudes are obtained from diagrams in imaginary time by continuing the euclidean p_0 for each external leg to $p_0 = -i\omega$. While the values of p_0 are discrete in imaginary time, $p_0 = \pi jT$ for integral j, in real time ω is a continuous variable. For hot field theories the two natural momentum scales are T, which we term "hard", and gT, which we call "soft". A momentum $P^\mu = (p_0, \boldsymbol{p})$ is soft if ω and $p = |\boldsymbol{p}|$ are of order gT; a momentum is hard if any component is of order T.

For hot gauge theories we term the diagrams which must be resummed into effective propagators and vertices "hard thermal loops". These are loop corrections which are g^2T^2/P^2 times the corresponding tree amplitude, where P is a momentum characteristic of the external lines. When any external leg is hard, these diagrams are at least g times the tree amplitude, and are part of the usual perturbative corrections. When every external momentum is soft, however,

g^2T^2/P^2 is of order 1, and hard thermal loops are as important as the tree diagram. Hard thermal loops are generated solely by a small part of the integration region in one-loop diagrams in which the loop momentum is hard.

For a scalar field theory the only hard thermal loop is the temperature-dependent mass in the self-energy, $m_s^2 \simeq g^2T^2$. The hard thermal loop in the photon self-energy of QED was computed decades ago by Silin [9, 10]. The hard thermal loops in the self-energies of nonabelian gauge theories were first computed by Klimov and Weldon [5, 10–12]. In sect. 2 we show that in gauge theories there are an infinite number of amplitudes with hard thermal loops: at any $N \geqslant 2$, there are hard thermal loops in the N-point functions between N gauge fields, and between a fermion pair and $N-2$ gauge fields. A further complication is that the hard thermal loops of gauge theories are produced not only by tadpole diagrams, but by diagrams with discontinuities. These discontinuities lie below the light-cone, $\omega \leqslant |\boldsymbol{p}|$, and represent Landau damping [4]. It is the occurrence of Landau damping that turns the hard thermal loops of gauge theories into nontrivial functions of the momenta.

The thermal contribution to tadpole diagrams and Landau discontinuities arise from the scattering off of particles in the thermal distribution. Thus hard thermal loops are due exclusively to thermal fluctuations; quantum fluctuations, such as the production of virtual particle–antiparticle pairs, do not enter. As a consequence, hard thermal loops are ultraviolet finite.

In order to systematically calculate amplitudes with soft lines, it is necessary to resum perturbation theory by including all possible hard thermal loops. For soft lines effective propagators must be used, in which the self-energies of Silin, Klimov and Weldon are included exactly. When every line going into a vertex is soft, an effective vertex, which includes the bare term plus the hard thermal loop, is required. If a line is hard, or if a vertex has at least one hard leg, loop corrections are suppressed by g, so bare propagators and vertices can be used to leading order in g. In particular, it is consistent to use bare propagators and vertices in order to calculate hard thermal loops.

The outline of the paper is as follows. In sect. 2 we show how to pick out the contributions of hard thermal loops from a diagram with soft external momenta. They arise from integration regions in which the loop momenta is hard. This allows us to make numerous approximations which greatly simplify the calculation of hard thermal loops.

The hard thermal loops of nonabelian gauge theories are computed in sect. 3. In subsect. 3.1 we work in Coulomb gauge. The hard thermal loops for two-, three-, and four-point functions are computed, and a generating functional for the hard thermal loops of arbitrary N-point functions is derived. We also show that the hard thermal loops satisfy particularly simple Ward identities. In subsect. 3.2 we show that the hard thermal loops are the same in Feynman gauge as in Coulomb gauge. The extension to general covariant gauges is made in subsect. 3.3. That the hard

thermal loops in the self-energies are gauge invariant was first shown by Klimov and Weldon [11, 12]. We argue inductively that these cancellations persist in all higher N-point functions. The gauge invariance of the hard thermal loops is surprising, for their external legs need *not* be on mass-shell – all that is required is that their legs be soft.

In subsect. 4.1 we develop an effective perturbative expansion which resums all hard thermal loops. We derive the Ward identities satisfied by the effective propagators and vertices, and find that they are *identical* in form to those satisfied at tree level. To illustrate the use of the effective expansion, in subsect. 4.2 we examine the leading corrections to the effective quark and gluon propagators. For soft momenta these corrections are of order g relative to the effective propagator. $\mathcal{T}$-matrix elements are formed by sandwiching these effective self-energies between physical wave functions, which are defined to lie on the mass-shells of the effective propagators. Ward identities are then used to show that these $\mathcal{T}$-matrix elements are the same in covariant and Coulomb gauges. In subsect. 4.3 we discuss the corrections at next to leading order in g.

Our proof in subsect. 4.2 that the two-point $\mathcal{T}$-matrix elements are gauge invariant implies that the damping rates are gauge invariant as well. Our proof of gauge invariance for $\mathcal{T}$-matrix elements extends the standard arguments at zero temperature [2] to our effective expansion, and provides a crucial check that our resummation includes all terms of order g. Also as at zero temperature, it is possible to show that the discontinuities can be written as a sum of amplitudes squared [14], which implies that the damping rates are positive.

In appendix A we compute one-loop integrals for three- and four-point functions.

This paper is the first in a series. In this paper we eschew explicit calculation to proceed as far as possible with general arguments such as power counting and the Ward identities. Detailed calculations of hard thermal loops, and applications to damping rates and other quantities, will be presented later [14]. We stress that while the effective expansion is not elementary, practical calculations can be performed with it. The principal complication – the nontrivial momentum dependence of the effective propagators and vertices – can be overcome by using spectral representations [5, 12, 14]. This is a straightforward extension of a standard nonconvariant method for evaluating loop integrals with bare propagators and vertices at nonzero temperature [4].

2. Extracting hard thermal loops

In this section we explain how to isolate the hard thermal loops in one-loop diagrams. We also enumerate all of the amplitudes which contain hard thermal loops and derive some useful identities.

Let $\Delta(K)$ be a bosonic propagator in momentum space,

$$\Delta(K) = 1/K^2, \qquad k^0 = 2\pi jT. \tag{2.1}$$

Upper-case letters represent four-momenta, lower-case letters their components: $K^\mu = (k^0, \boldsymbol{k})$, with $\boldsymbol{k} = k\hat{\boldsymbol{k}}$, and $K^2 = (k^0)^2 + k^2$. For one-loop diagrams we take K^μ as the loop momenta, with

$$\mathrm{Tr} = T \sum_{j=-\infty}^{+\infty} \int \mathrm{d}^3k/(2\pi)^3. \tag{2.2}$$

To perform the sum over the integers j at nonzero temperature we follow the method of refs. [4, 13]. This "noncovariant" approach uses propagators that depend upon the spatial momentum $\boldsymbol{k}$ and the euclidean time τ. The noncovariant propagator is obtained by Fourier transformation of $\Delta(K)$ with respect to k^0,

$$\Delta(\tau, k) = T \sum_{\substack{j=-\infty, \\ k^0 = 2\pi jT}}^{+\infty} \mathrm{e}^{-ik^0\tau}\Delta(K). \tag{2.3}$$

The sum can be evaluated by expressing it as a contour integral [4, 5, 12]. In the complex k^0-plane $\Delta(K)$ has poles at $k^0 = \pm ik$ with residues $\mp i/2k$. The contour integral gives

$$\Delta(\tau, k) = (1/2k)\big((1 + n(k))\mathrm{e}^{-k\tau} + n(k)\mathrm{e}^{+k\tau}\big), \tag{2.4}$$

where $n(k) = 1/(\exp(k/T) - 1)$ is the Bose–Einstein distribution function. Eq. (2.4) is valid for $0 \leqslant \tau \leqslant 1/T$; outside this region, $\Delta(\tau, k)$ is defined to be periodic in τ with period $1/T$. The inverse of eq. (2.3) is

$$\Delta(K) = \int_0^{1/T} \mathrm{d}\tau\, \mathrm{e}^{ik^0\tau}\Delta(\tau, k). \tag{2.5}$$

Similar results apply for the quark propagator $\Delta_{\mathrm{f}}(K)$. We find it useful to define a fermionic propagator $\tilde{\Delta}(K)$ by extracting a $\not{K}$ from the quark propagator,

$$\Delta_{\mathrm{f}}(K) = i/\not{K} = i\not{K}\tilde{\Delta}(K). \tag{2.6}$$

$\tilde{\Delta}(K)$ differs from $\Delta(K)$ only in the allowed values of k^0:

$$\tilde{\Delta}(K) = 1/K^2, \qquad k^0 = (2j + 1)\pi T. \tag{2.7}$$

The noncovariant propagator $\tilde{\Delta}(\tau, k)$ is defined as in eq. (2.3), except for the

change in the values of k^0. After evaluating the sum over j by contour integral methods, we obtain

$$\tilde{\Delta}(\tau,k) = (1/2k)\big((1-\tilde{n}(k))e^{-k\tau} - \tilde{n}(k)e^{+k\tau}\big), \tag{2.8}$$

with $\tilde{n}(k) = 1/(\exp(k/T)+1)$ the Fermi–Dirac distribution function. Eq. (2.8) holds over $0 \leqslant \tau \leqslant 1/T$; otherwise it is defined to be antiperiodic in τ with period $1/T$. Note that $\tilde{\Delta}(\tau,k)$ is obtained from $\Delta(\tau,k)$ by replacing $n(k) \to -\tilde{n}(k)$.

In the noncovariant approach [4,5,12] one-loop integrals are evaluated as follows. Start with the expression for the diagram in momentum space. For each virtual line use eq. (2.5) (or the analogous relation for $\tilde{\Delta}(K)$) to replace the propagator $\Delta(K)$ by an integral of $\Delta(\tau,k)$ with respect to τ. The sum over k^0 produces a δ function in the times τ, allowing one τ integral to be done trivially. The integrals over the remaining times are elementary, and yield products of energy denominators. This leaves an integral over the three-momentum $\boldsymbol{k}$. At this point it is relatively easy to pick out the contribution of the hard thermal loops. As noted in sect. 1, hard thermal loops are g^2T^2/P^2 times the corresponding tree diagram: for one-loop diagrams the g^2 is automatic, so the integrals that produce hard thermal loops are uniformly proportional to T^2.

To illustrate this procedure we compute several examples. We begin with the simplest diagram which produces a hard thermal loop, which is the tadpole diagram for bosons, $\mathrm{Tr}\,\Delta(K)$. After using eq. (2.5) the sum over k^0 just gives $\delta(\tau)$, so the τ integral is trivial:

$$\mathrm{Tr}\,\Delta(K) = \int \frac{d^3k}{(2\pi)^3}\Delta(\tau=0,k) = \int \frac{d^3k}{(2\pi)^3}\frac{1}{2k}(1+2n(k)). \tag{2.9}$$

The first term in the integral is quadratically divergent, and is removed by renormalization at zero temperature. In the second term the quadratic divergence is cutoff by the Bose–Einstein distribution function $n(k)$. Using

$$\int_0^{+\infty} dk\,k\,n(k) = \tfrac{1}{6}\pi^2T^2, \tag{2.10}$$

we find that the hard thermal loop in this integral – the term proportional to T^2 – is

$$\mathrm{Tr}\,\Delta(K) \approx \tfrac{1}{12}T^2 = \mathscr{J}(0). \tag{2.11}$$

We introduce the symbol "$\approx$" to represent equality between the hard thermal loops in two expressions. We also introduce the notation $\mathscr{J}(P) = \mathscr{J}(0)$ for the hard thermal loop in $\mathrm{Tr}\,\Delta(K-P)$. Later this will be generalized into a compact notation for the hard thermal loops in more complicated integrals.

The quark loop in the gluon self-energy also contributes a type of fermionic tadpole, $\mathrm{Tr}\,\tilde{\Delta}(K)$. Using

$$\int_0^{+\infty} \mathrm{d}k\, k\, \tilde{n}(k) = \left(\tfrac{1}{2}\right)\tfrac{1}{6}\pi^2 T^2 , \tag{2.12}$$

we find

$$\mathrm{Tr}\,\tilde{\Delta}(K) \approx -\tfrac{1}{24}T^2 = \tilde{\mathscr{J}}(0) . \tag{2.13}$$

Note the identity

$$\tilde{\mathscr{J}}(0) = -\tfrac{1}{2}\mathscr{J}(0) , \tag{2.14}$$

which generalizes to more complicated integrals.

A more interesting example of a hard thermal loop is $\mathrm{Tr}\,k^2\Delta(K)\Delta(P-K)$. This arises in the gluon self-energy $\Pi^{\mu\nu}$, when traced over its spatial indices $\mu = \nu = i$. After using eq. (2.5) and eliminating one τ integral,

$$\mathrm{Tr}\,k^2\Delta(K)\Delta(P-K) = \int \frac{\mathrm{d}^3k}{(2\pi)^3}\int_0^{1/T} \mathrm{d}\tau\, \mathrm{e}^{ip^0\tau} k^2\Delta(\tau, E_k)\Delta(\tau, E_{p-k}) , \tag{2.15}$$

where $E_k = k$, $E_{p-k} = |\boldsymbol{p}-\boldsymbol{k}|$. The remaining τ integral yields a set of energy denominators,

$$\begin{aligned}
&\mathrm{Tr}\,k^2\Delta(K)\Delta(P-K) \\
&= \int \frac{\mathrm{d}^3k}{(2\pi)^3}\frac{k^2}{2E_k 2E_{p-k}}\left\{\left(1+n(E_k)+n(E_{p-k})\right)\left(\frac{-1}{ip^0-E_k-E_{p-k}}\right.\right. \\
&\qquad \left.\left. + \frac{1}{ip^0+E_k+E_{p-k}}\right) - \left(n(E_k)-n(E_{p-k})\right)\left(\frac{-1}{ip^0-E_k+E_{p-k}} + \frac{1}{ip^0+E_k-E_{p-k}}\right)\right\}
\end{aligned} \tag{2.16}$$

In passing from eq. (2.15) to eq. (2.16) p^0 must be treated as a euclidean variable, $p^0 = 2\pi jT$, with $\exp(ip^0/T) = 1$. Once the integral is written as a sum over energy denominators, though, we can analytically continue p^0 to Minkowski values, $p^0 = -i\omega$. For soft P^μ (ω and p both of order gT) the hard thermal loop can be extracted by power counting.

By definition the hard thermal loop in the self-energy $\Pi^{\mu\nu}$ is the piece which is as large as the tree term for soft momentum. The transverse part of the bare inverse propagator is $P^2\delta^{\mu\nu} - P^\mu P^\nu$: at soft $P \sim gT$ this is of order g^2T^2. Since the integral in eq. (2.16) is multiplied by g^2 in $\Pi^{\mu\nu}$, the hard thermal loop in the integral is the term proportional to T^2, as stated before. We now extract this term.

The 1 in the expression $1 + n(E_k) + n(E_{p-k})$ in eq. (2.16) generates the complete integral at zero temperature. After renormalization removes the ultraviolet divergence, this contribution to the integral in eq. (2.16) is proportional to P^2, which at soft P is of magnitude g^2T^2. This illustrates a general feature: for soft momenta, the zero temperature terms are down by g^2 relative to the hard thermal loops.

The other terms in eq. (2.16) involve the statistical distribution functions $n(E_k)$ or $n(E_{p-k})$. We first consider soft loop momentum $\boldsymbol{k}$. If the external momentum P^μ is soft, the integral over magnitude, $\int dk$, is mixed up with the angular integral, $\int d\Omega$, and they are complicated to evaluate. It is not difficult, though, to estimate how large this part of the integral is. For soft energies E of order gT, the Bose–Einstein distribution function is approximately

$$n(E) \simeq T/E \sim 1/g . \tag{2.17}$$

When the external and loop momentum are both soft, the only mass scale in the integral is gT, so that the contribution to the integral is of order $n(E)(gT)^2 \sim gT^2$, which is suppressed by g relative to the hard thermal loop.

All that remains is the integration over hard loop momentum. There are significant simplifications when P is soft and k hard. In the energy denominators we can approximate

$$ip^0 \pm (E_k + E_{p-k}) \simeq \pm 2k, \qquad ip^0 \pm (E_k - E_{p-k}) \simeq ip^0 \pm p\cos\theta , \tag{2.18}$$

where θ is the angle between $\boldsymbol{p}$ and $\boldsymbol{k}$. For the distribution functions we can set

$$\begin{aligned} n(E_k) + n(E_{p-k}) &\simeq 2n(k) , \\ n(E_k) - n(E_{p-k}) &\simeq -\frac{p\cos\theta}{T} n(k)(1+n(k)) . \end{aligned} \tag{2.19}$$

With these approximations, the integrals over $\int dk$ and $\int d\Omega = \int \sin\theta \, d\theta \, d\phi$ decouple, and each can easily be done. The k integral is either that given in eq. (2.10), or

$$\frac{1}{T}\int_0^\infty dk\, k^2 n(k)(1+n(k)) = \tfrac{1}{3}\pi^2 T^2 . \tag{2.20}$$

For later use, we also give the corresponding integral for $\tilde{n}(k)$,

$$\frac{1}{T}\int_0^\infty dk\, k^2 \tilde{n}(k)(1-\tilde{n}(k)) = \left(\tfrac{1}{2}\right)\tfrac{1}{3}\pi^2 T^2 . \tag{2.21}$$

Under the approximations of eqs. (2.18) and (2.19), the angular integral over

$x = \cos\theta$ reduces to

$$\int_{-1}^{1} \frac{x\,\mathrm{d}x}{ip^0/p - x} = 2Q_1\left(\frac{ip^0}{p}\right) = \frac{ip^0}{p}\log\left(\frac{ip^0+p}{ip^0-p}\right) - 2, \tag{2.22}$$

where $Q_1(ip^0/p)$ is a Legendre function of the second kind.

The final result for the hard thermal loop in eq. (2.15) is

$$\mathrm{Tr}\, k^2 \Delta(K)\Delta(P-K) \approx \frac{T^2}{24}\left(1 - 2Q_1\left(\frac{ip^0}{p}\right)\right) = \mathscr{J}^{ii}(0,P)\,. \tag{2.23}$$

We introduce the notation $\mathscr{J}^{\mu\nu}(P_0, P_1)$ for the hard thermal loop in the integral $\mathrm{Tr}\, K^\mu K^\nu \Delta(P_0 - K)\Delta(P_1 - K)$. The denominators $ip^0 \pm (E_k + E_{p-k})$ in eq. (2.16) produce the constant term, $T^2/24$, which is like the tadpole integral of eq. (2.11). The term containing $Q_1(ip^0/p)$ is due to the denominators $ip^0 \pm (E_k - E_{p-k})$. The Legendre functions $Q_n(\omega/p)$ have discontinuities below the light-cone, $p > \omega > -p$. These terms represent Landau damping at nonzero temperature, where one field is absorbed from the thermal distribution, and the other emitted into it [4, 5, 9–12].

As a third example of a hard thermal loop, consider an integral which enters into the quark self-energy, $\mathrm{Tr}\, k^0 \Delta(K)\tilde{\Delta}(P-K)$. After summation over k^0 and integration over τ, the integral becomes

$$\begin{aligned}
&\mathrm{Tr}\, k^0 \Delta(K)\tilde{\Delta}(P-K) \\
&= \int \frac{\mathrm{d}^3k}{(2\pi)^3} \frac{-iE_k}{2E_k 2E_{p-k}} \left\{ \left(1 + n(E_k) - \tilde{n}(E_{p-k})\right)\left(\frac{-1}{ip^0 - E_k - E_{p-k}} + \frac{-1}{ip^0 + E_k + E_{p-k}}\right)\right. \\
&\qquad \left. + \left(n(E_k) + \tilde{n}(E_{p-k})\right)\left(\frac{1}{ip^0 - E_k + E_{p-k}} + \frac{1}{ip^0 + E_k - E_{p-k}}\right)\right\}.
\end{aligned} \tag{2.24}$$

The hard thermal loop is the term that is as large as the bare inverse propagator, $\not{P}$, for soft momentum $P \sim gT$. In the quark self-energy Σ, the integral in eq. (2.24) is multiplied by g^2, so the hard thermal part of the integral is proportional to T^2/P. Such a term is produced only by the two terms in eq. (2.24) with energy denominators $ip^0 \pm (E_k - E_{p-k})$, integrated over hard momenta $k \sim T$. Using the approximations in eqs. (2.18) and (2.19), the integral over k decouples from the angular integral, with the k integral given by either eqs. (2.10) or (2.12). The

angular integral has the form

$$\int_{-1}^{1} \frac{\mathrm{d}x}{ip^0/p - x} = 2Q_0\left(\frac{ip^0}{p}\right) = \log\left(\frac{ip^0+p}{ip^0-p}\right). \tag{2.25}$$

The final result for the hard thermal loop in the integral is

$$\mathrm{Tr}\, k^0 \Delta(K)\tilde{\Delta}(P-K) \approx -i\frac{T^2}{16p}Q_0\left(\frac{ip^0}{p}\right) = \mathscr{J}^0(0;P). \tag{2.26}$$

We have denoted the hard thermal part of $\mathrm{Tr}\, K^\mu \Delta(P_0-K)\tilde{\Delta}(P_1-K)$ by $\mathscr{J}^\mu(P_0;P_1)$. The other parts of the integral in eq. (2.24) are all smaller by at least one power of g. At hard k the energy denominators $ip^0 \pm (E_k + E_{p-k})$ produce terms in the integral proportional to T, and are therefore of order g times the hard thermal loop. The integral over soft k is also of order g, while the zero temperature term is of order g^2 times the hard thermal loop.

We have shown how to extract the hard thermal loops in a few simple integrals. Before proceeding to the general case, we first list all diagrams which contain hard thermal loops. In nonabelian gauge theories the only amplitudes which contain hard thermal loops are N-gluon amplitudes and the amplitude between $N-2$ gluons and a quark pair. In Coulomb or Feynman gauges, hard thermal loops are produced by a very small subset of one-loop diagrams. They arise just from diagrams constructed out of three-point vertices, as in figs. 1 and 2. As we show in sect. 3, in these gauges any diagram with a four-gluon vertex cannot produce a hard thermal loop. There is one exception to this rule: for the gluon self-energy, the four-gluon vertex produces a tadpole diagram, which by eq. (2.11) contains a hard thermal loop.

This neglect of diagrams with four-gluon vertices holds only in Coulomb and Feynman gauges. As we demonstrate in subsect. 3.3, in covariant gauges other than Feynman, the full set of one-loop diagrams contributes to hard thermal loops. When every one-loop diagram which contributes to a given amplitude is added up, however, we find that the sum gives the same hard thermal loop as found in Coulomb or Feynman gauge. For the sake of simplicity, in the rest of this section we restrict ourselves to Coulomb or Feynman gauge.

In nonabelian gauge theories, diagrams are often difficult to evaluate because in the numerators of integrals, the external and loop momenta become entangled. These complications are avoided in hard thermal loops. As in the previous examples, hard thermal loops arise from integration regions in which the loop momentum K is hard, while all external momenta are soft. If in the numerator of an integral a hard loop momentum of order T is replaced by a soft external momentum of order gT, this substitution reduces the integral by a power of g.

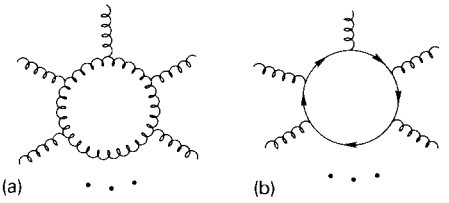

Fig. 1. Diagrams which contribute to the hard thermal loop of the N-gluon amplitude in Coulomb gauge.

Thus whenever a momentum appears in the numerator, such as $(P-K)^\mu$ from a three-gluon vertex, or $\not{P}-\not{K}$ from a quark propagator, we need only keep the loop momentum K, dropping all terms proportional to the external momenta. Another simplification is that hard thermal loops are only produced by terms in which every external gluon has its space-time index μ tied to a loop momentum K^μ; that is, terms proportional to Kronecker deltas in the indices between external gluons, $\delta^{\mu\nu}$, can be dropped. This simplification arises from an identity, eq. (2.33), satisfied by hard thermal loops. Again the gluon self-energy is an exception: it does have hard thermal loops proportional to $\mathscr{I}(0)\delta^{\mu\nu}$ and $\tilde{\mathscr{I}}(0)\delta^{\mu\nu}$.

Using these rules, we catalog all diagrams which have hard thermal loops in Coulomb and Feynman gauges. For the N-gluon amplitude, N gluons can tie onto a gluon loop through the one-loop diagram of fig. 1a. This produces the hard thermal loop

$$\mathscr{I}^{\mu_1\cdots\mu_N}(0,P_1,\ldots,P_{N-1}) \approx \mathrm{Tr}\, K^{\mu_1}\ldots K^{\mu_N}\Delta(K)\Delta(P_1-K)\ldots\Delta(P_{N-1}-K)\,, \tag{2.27}$$

where $\mu_1,\ldots,\mu_N$ are the indices of the external gluons, and $P_1,\ldots,P_{N-1}$ are combinations of their momenta. Recall that the symbol "$\approx$" indicates that $\mathscr{I}^{\mu_1\cdots\mu_N}$ is defined to be the hard thermal loop in the integral. The N powers of K in the numerator arise from the N three-gluon vertices in fig. 1a. In Feynman gauge, the diagram in which N gluons attach to a ghost loop also contribute a hard thermal loop like eq. (2.27). The hard thermal loop calculated in eq. (2.23) is a special case of eq. (2.27). The N gluons can also be tied onto a quark loop as in fig. 1b, to give the hard thermal loop

$$\tilde{\mathscr{I}}^{\mu_1\cdots\mu_N}(0,P_1,\ldots,P_{N-1}) \approx \mathrm{Tr}\, K^{\mu_1}\ldots K^{\mu_N}\tilde{\Delta}(K)\tilde{\Delta}(P_1-K)\ldots\tilde{\Delta}(P_{N-1}-K)\,. \tag{2.28}$$

The powers of K in this integral arise from the $\not{K}$'s in the N quark propagators. These are all of the hard thermal loops in the N-gluon amplitude for $N \geqslant 3$. As

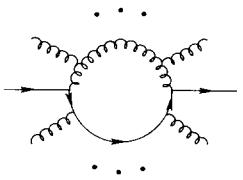

Fig. 2. Diagrams which contribute to the hard thermal loop of the amplitude between a quark pair and $(N-2)$ gluons in Coulomb gauge.

noted above, the gluon self-energy, $N=2$, provides exceptions to these rules. This case is discussed at length in sect. 3.

The hard thermal loops for amplitudes with $(N-2)$ gluons and a quark pair arise from the diagrams of fig. 2. The integrals are of the form

$$\mathcal{J}^{\mu_1\cdots\mu_{N-1}}(0,P_1,\ldots,P_{M-1};P_M,\ldots,P_{N-1})$$

$$\approx \mathrm{Tr}\,K^{\mu_1}\ldots K^{\mu_{N-1}}\Delta(K)\ldots\Delta(P_{M-1}-K)\tilde{\Delta}(P_M-K)\ldots\tilde{\Delta}(P_{N-1}-K)\,, \quad (2.29)$$

where M can take any value from 1 to $N-1$, and $P_1,\ldots,P_{N-1}$ are combinations of the external momenta. The indices of the external gluons are $\mu_1,\ldots,\mu_{N-2}$; the additional index, μ_{N-1}, is contracted with a Dirac gamma matrix, $\gamma^{\mu_{N-1}}$. In the arguments of eq. (2.29), the momenta that appear in bosonic propagators are separated by a semicolon from those that appear in fermionic propagators. Note that there are only $N-1$ powers of K in eq. (2.29), versus N powers of K in eqs. (2.27) and (2.28). The hard thermal loop calculated in eq. (2.26) is a special case of eq. (2.29), for $N=2$ and $M=1$. The hard thermal loops in eq. (2.29) exist for all $N\geqslant 2$.

In nonabelian gauge theories these are the only integrals which develop hard thermal loops. To justify this we develop a set of rules which enables us to power count one-loop diagrams. In appendix A we explicitly evaluate the sum over k^0 and the integrals over τ for the three- and four-point functions. From these examples, the general form of the corresponding result for an N-point function is apparent. To be definite, consider the integral in eq. (2.27), taking all of the indices $\mu_1,\ldots,\mu_N$ to be spatial (this restriction is not essential, and is lifted later). In the noncovariant approach, eq. (2.5) is used to introduce a τ integral for each of the N propagators. The sum over k^0 produces a delta function in the τ's, which eliminates one τ integral. Each of the remaining $(N-1)$ τ integrals then gives an energy denominator.

At this point we invoke a general property of one-loop diagrams, which seems to have escaped notice before. By eq. (2.4), each propagator can contribute one power of the Bose–Einstein distribution function $n(E)$ to the integral. For the integral in eq. (2.27), since there are N propagators, at the outset there will be

terms involving N powers of the distribution functions. Yet after doing the sum over k^0 and the integrals over each τ, we assert that any one-loop integral can be written in a form in which there are at most single powers of the distribution functions: all higher powers in the $n(E)$'s cancel. This property is demonstrated explicitly in appendix A for arbitrary three- and four-point functions. We also give a physical argument as to why this property holds for any N-point function, as a consequence of the way in which the cutting rules work at nonzero temperature.

Using this result, we reduce the integral in eq. (2.27) to a sum which includes terms of the form

$$\int \mathrm{d}^3k \frac{K^{\mu_1} \ldots K^{\mu_N}}{E_k E_{p_1-k} \ldots E_{p_{N-1}-k}} \left(n(E_k) - n(E_{p_1-k})\right) \times \left[\left(ip_1^0 - E_k + E_{p_1-k}\right) \ldots \left(ip_{N-1}^0 - E_k + E_{p_{N-1}-k}\right)\right]^{-1}. \tag{2.30}$$

The N factors of $1/E_{p-k}$ arise from the residues of the propagators. Each energy denominator corresponds to a way in which the one-loop diagram can be cut through two virtual lines to produce a discontinuity. For the term shown in eq. (2.30), in every denominator the two energies have opposite signs. Consequently, for eq. (2.30) any possible cut corresponds to Landau damping: the absorption and emission of two particles, with nearly equal momenta, from the thermal bath. For the other terms in the integral, the energies in the denominators have different signs, and different combinations of the distribution functions appear.

Hard thermal loops arise from the integration region in which k is of order T. Using the approximations of eqs. (2.18) and (2.19), it is simple to estimate the magnitude of eq. (2.30) when the external momenta are of order gT. In the integral over $\int \mathrm{d}^3k$, the N powers of K in the numerator, and the N residues, $E_{p-k} \simeq k$, are all proportional to T, and combine with the integration element to give $T^3T^N/T^N = T^3$. By eq. (2.19), the difference of distribution functions is of order P/T. Finally, from eq. (2.18) each energy denominator is of order P. Altogether, eq. (2.30) is of order T^2/P^{N-2}. In the N-gluon amplitude, eq. (2.30) is multiplied by g^N, giving $g^N T^2/P^{N-2} = (g^2T^2/P^2)g^{N-2}/P^{N-4}$. At tree level the N-gluon amplitude is of order g^{N-2}/P^{N-4}. For soft $P \sim gT$, eq. (2.30) is of the same order and so produces a hard thermal loop.

There is one other type of term which produces a hard thermal loop from the integral of eq. (2.27). Consider the term in which every energy denominator except one corresponds to Landau damping, so one energy denominator is of order T. The statistical distribution functions for that energy denominator appear as a sum, and are of order 1. The result is that such a term also gives a hard thermal loop. Only these two types of terms produce a hard thermal loop: all others are smaller by at least one power of g. Note that if N is large, these two types of terms are a

small fraction of the total number of terms. The analysis of the integral in eq. (2.28) is identical, except that the Bose–Einstein distribution functions $n(E)$ must be replaced by Fermi–Dirac distribution functions $\tilde{n}(E)$ everywhere.

The analysis of the integral in eq. (2.29) is similar. After evaluating all the τ integrals, the integral includes terms like

$$\int \mathrm{d}^3k \frac{K^{\mu_1} \cdots K^{\mu_{N-1}}}{E_k E_{p_1-k} \cdots E_{p_{N-1}-k}} \left(n(E_k) + \tilde{n}\left(E_{p_{N-1}-k}\right)\right)$$

$$\times \left[\left(ip_1^0 - E_k + E_{p_1-k}\right) \cdots \left(ip_{N-1}^0 - E_k + E_{p_{N-1}-k}\right)\right]^{-1}. \qquad (2.31)$$

In this term, all energy denominators correspond to Landau damping; thus the statistical distribution functions which appear must be the sum of $n(E)$ and $\tilde{n}(E)$. The integral is estimated as before, except that the sum of distribution functions is of order 1. We find that eq. (2.31) is of order T^2/P^{N-1}; it contributes to the amplitude for $N-2$ gluons and a quark pair as $g^N T^2/P^{N-1} = (g^2T^2/P^2)g^{N-2}/P^{N-3}$. The amplitude at tree level is of order g^{N-2}/P^{N-3}, so eq. (2.31) contributes to the hard thermal loop.

For the integral of eq. (2.29) only terms in which every energy denominator corresponds to Landau damping, as in eq. (2.31), produce hard thermal loops. Observe that while the integral in eq. (2.29) has one fewer power of K in the numerator than eqs. (2.27) and (2.28), it is still a hard thermal loop. This happens because the distribution functions which enter into eq. (2.30) are of the same statistics, so their difference is of order P/T. In eq. (2.31) they are of opposite statistics, so their sum is of order 1. This change in the distribution functions compensates for the one fewer power of K in the numerator.

These results can be summarized by a set of rules for power counting one-loop diagrams. We assume that all external momentum are soft, denoted generically by P.

(i) The integration element $\int \mathrm{d}^3k$ contributes T^3.

(ii) The first propagator in the integral, times the sum over k^0, contributes $1/T$.

(iii) Every additional propagator gives $1/PT$: $1/T$ from the residue times $1/P$ from an energy denominator with Landau damping.

(iv) Powers of K^μ in the numerator from three-gluon vertices or quark propagators give T, powers of external momenta give P.

(v) For integrals with two or more propagators that are either all bosonic or all fermionic, there is an extra factor of P/T from cancelling statistical distribution functions.

In the above, by propagator we mean either Δ or $\tilde{\Delta}$; as discussed in subsect. 3.1, the power counting for static modes is different.

These rules apply to diagrams in which every external momentum is soft. If each external momentum is hard, then as T is the only scale in the problem, by dimensional analysis any one-loop diagram is g^2 times the tree amplitude. The case in which some external momenta are hard, and some soft, is more involved. Suppose an amplitude has two external lines with hard momenta, while the rest are soft. The largest loop diagrams are those in which the hard momenta is routed through just one virtual line. For the propagator of this hard virtual line, the associated energy denominator is hard, of order $1/T$, instead of soft, of order $1/P$. The only other change in the rules is that there is no suppression from cancelling statistical distribution functions. The result is that one-loop diagrams with both hard and soft external momenta are at most g times the tree amplitude. For example, consider the amplitude between three gluons, where two of the gluons have hard momenta, of order Q, and one gluon has soft momenta, of order P. At tree level this is of order $gQ \sim gT$. By the counting above there are diagrams of order $g^3T^2/P \sim g^2T$, which for hard Q is g times the tree amplitude.

The amplitudes discussed, between N gluons, and between $N-2$ gluons and a quark pair, are the only ones with hard thermal loops. We leave it as an exercise to the reader to show that amplitudes with more than one quark pair do not have hard thermal loops. The only remaining amplitudes involve ghosts. In gauges in which ghosts propagate – such as covariant – virtual ghosts do contribute to hard thermal loops. It is always true, however, that amplitudes with ghosts on external lines do not exhibit hard thermal loops. For instance, in the one-loop diagram between one pair of ghosts and $N-2$ gluons, one ghost–gluon vertex is proportional to an external ghost momentum. Assuming that all of the external momenta are soft, this ghost–gluon vertex brings in one power of a soft external momentum, instead of a hard loop momentum. Hence the amplitude with one ghost pair and $N-2$ gluons is at most g times the one-loop amplitude between N gluons.

We conclude this section by deriving some useful identities for hard thermal loops. The integrals of eqs. (2.27) and (2.28) are evidently invariant under permutations of their arguments $P_0 = 0, P_1, \ldots, P_{N-1}$ while eq. (2.29) is invariant under permutations of $P_0 = 0, P_1, \ldots, P_{M-1}$ and $P_M, \ldots, P_{N-1}$ amongst themselves.

All arguments can be shifted by a common soft momentum P. For example,

$$\mathscr{J}^{\mu_1 \cdots \mu_N}(P_0, \ldots, P_{N-1}) = \mathscr{J}^{\mu_1 \cdots \mu_N}(P_0 + P, \ldots, P_{N-1} + P) . \qquad (2.32)$$

We often use this freedom to set $P_0 = 0$. To prove this identity, we change the integration variable in eq. (2.27) from K to $K - P$. In the numerator, every K^μ becomes $(K-P)^\mu$, but in the hard thermal loop any factor of the soft P can be dropped. Remember that the functions $\mathscr{J}$ and $\tilde{\mathscr{J}}$ are defined to include only the hard thermal loops in the integrals of eqs. (2.27)–(2.29); thus identities such as eq. (2.32), and those which follow, are strict equalities.

The integrals in eqs. (2.27)–(2.29) are symmetric under permutation of their indices. For $N \geqslant 3$, the integral $\mathscr{J}^{\mu_1 \cdots \mu_N}$ is traceless in any pair of indices:

$$\delta^{\mu_1\mu_2} \mathscr{J}^{\mu_1\mu_2 \cdots \mu_N}(0, P_1, \ldots, P_{N-1}) = 0, \qquad N \geqslant 3, \tag{2.33}$$

and similarly for the integrals in eqs. (2.28) and (2.29). The reason is that $\delta^{\mu_1\mu_2} K^{\mu_1} K^{\mu_2} = K^2$ cancels $\Delta(K)$ in eq. (2.27), leaving an integral with $N-2$ factors of K in the numerator and $N-1$ propagators. From our rules for power counting, this integral is of order T/P^{N-3}, which is not a hard thermal loop. As described earlier, this identity allows us to drop terms with Kronecker deltas in the indices between external gluons, for if two external indices are contracted together, then two internal indices must be contracted as well.

When $N = 2$ the integrals of eqs. (2.27) and (2.28) have nonzero trace:

$$\delta^{\mu\nu} \mathscr{J}^{\mu\nu}(0, P) = \mathscr{J}(P) = \mathscr{J}(0), \tag{2.34}$$

where $\mathscr{J}(0)$ is given in eq. (2.11).

The identity of eq. (2.33) is also useful for calculating integrals where more than one of the indices $\mu_1 \ldots \mu_N$ is timelike. After introducing noncovariant propagators, k^0 becomes $i\partial/\partial\tau$. Single powers of $\partial/\partial\tau$ can be integrated by parts without concern, but care must be taken with multiple powers of $\partial/\partial\tau$ [4]. Hard thermal loops with multiple powers of k^0 can be evaluated by writing eq. (2.33) as

$$\mathscr{J}^{00\mu_3 \cdots \mu_N}(0, P_1, \ldots, P_{N-1}) = -\mathscr{J}^{ii\mu_3 \cdots \mu_N}(0, P_1, \ldots, P_{N-1}). \tag{2.35}$$

With this identity the previous restriction that the indices $\mu_1, \ldots, \mu_N$ all be spatial can be lifted.

There are also identities which relate hard thermal loops for propagators with different statistics. To start with, the hard thermal loops in eqs. (2.27) and (2.28) are equal up to a multiplicative constant. Consider the contribution to the hard thermal loop in eq. (2.27) from terms as in eq. (2.30). To obtain the similar hard thermal loop for eq. (2.28), merely replace $n(E)$ by $-\tilde{n}(E)$ in eq. (2.30). From eqs. (2.10), (2.12), (2.20) and (2.21), this substitution changes the integrals over $\int \mathrm{d}k$ by an overall multiplicative factor of $-\frac{1}{2}$. This same $-\frac{1}{2}$ accompanies the other terms which contribute to a hard thermal loop, so in all

$$\tilde{\mathscr{J}}^{\mu_1 \cdots \mu_N}(0, P_1, \ldots, P_{N-1}) = \left(-\tfrac{1}{2}\right) \mathscr{J}^{\mu_1 \cdots \mu_N}(0, P_1, \ldots, P_{N-1}). \tag{2.36}$$

Eq. (2.14) is an example of this identity.

There is another type of identity which relates eq. (2.29) to similar integrals. Define the integral which is obtained from eq. (2.29) by changing each Δ into $\tilde{\Delta}$,

and vice versa, as $\tilde{\mathscr{J}}$:

$$\tilde{\mathscr{J}}^{\mu_1\cdots\mu_{N-1}}(0,P_1,\ldots,P_{M-1};P_M,\ldots,P_{N-1})$$

$$\approx \mathrm{Tr}\,K^{\mu_1}\ldots K^{\mu_{N-1}}\tilde{\Delta}(K)\ldots\tilde{\Delta}(P_{M-1}-K)\Delta(P_M-K)\ldots\Delta(P_{N-1}-K)\,. \quad (2.37)$$

As seen in eq. (2.31), the only statistical distributions functions which enter into the hard thermal loop of eq. (2.29) are $\tilde{n}(E_k)+n(E_{p_{N-1}-k})\simeq\tilde{n}(k)+n(k)$. To obtain the hard thermal loop for eq. (2.37), in eq. (2.31) each $n(E)$ is replaced by $-\tilde{n}(E)$, and vice versa. Under this operation, $\tilde{n}(k)+n(k)$ goes into minus itself, so that

$$\tilde{\mathscr{J}}^{\mu_1\cdots\mu_{N-1}}(0,P_1,\ldots,P_{M-1};P_M,\ldots,P_{N-1})$$

$$=-\mathscr{J}^{\mu_1\cdots\mu_{N-1}}(0,P_1,\ldots,P_{M-1};P_M,\ldots,P_{N-1})\,. \quad (2.38)$$

Finally we derive relations between the hard thermal loops of N- and $(N-1)$-point functions. For soft P_1 we can approximate

$$P_1^\mu K^\mu=\tfrac{1}{2}\big(-(P_1-K)^2+K^2+P_1^2\big)\simeq\tfrac{1}{2}\big(-(P_1-K)^2+K^2\big)\,. \quad (2.39)$$

Each of the terms K^2 and $(P_1-K)^2$ cancels a propagator in eq. (2.27), so

$$P_1^{\mu_1}\mathscr{J}^{\mu_1\mu_2\cdots\mu_N}(0,P_1,P_2,\ldots,P_{N-1})$$

$$=\tfrac{1}{2}\big(\mathscr{J}^{\mu_2\cdots\mu_N}(P_1,P_2,\ldots,P_{N-1})-\mathscr{J}^{\mu_2\cdots\mu_N}(0,P_2,\ldots,P_{N-1})\big)\,. \quad (2.40)$$

For $N=2$, this can be further simplified:

$$P^\mu\mathscr{J}^{\mu\nu}(0,P)=\tfrac{1}{2}\big(\mathscr{J}^\nu(P)-\mathscr{J}^\nu(0)\big)=\tfrac{1}{2}P^\nu\mathscr{J}(0)\,. \quad (2.41)$$

Here we use $\mathscr{J}^\nu(0)=\mathrm{Tr}\,K^\nu\Delta(K)=0$ because the integral is odd in K^ν, and $\mathscr{J}^\nu(P)=P^\nu\mathscr{J}(0)$ follows from shifting $K\to K+P$. An identity similar to eq. (2.40) can be derived for eq. (2.29).

Eq. (2.40) shows that for $N\geqslant 3$ a soft momentum dotted into an N-point hard thermal loop yields a difference of two $(N-1)$-point hard thermal loops. In subsect. 3.1 we use eqs. (2.40) and (2.41) to derive the Ward identities satisfied by hard thermal loops.

3. Hard thermal loops in hot gauge theories

For hot gauge theories in Coulomb and Feynman gauge, the hard thermal loops can be expressed in terms of the integrals $\mathscr{J}$ and $\tilde{\mathscr{J}}$ of sect. 2. In this section we prove a surprising result: at least within the class of Coulomb and general covariant gauges, all hard thermal loops are gauge invariant.

Our conventions for perturbation theory are the following. We work in an $SU(N_c)$ gauge theory with N_f flavors of fermions in the fundamental representation. The color indices $a, b, \ldots$ run from 1 to $N_c^2 - 1$, while the (euclidean) space-time indices $\mu, \nu, \ldots$ run from 1 to d. We work in four space-time dimensions, $d = 4$, but on occasion we find it useful to keep d as a bookkeeping device. Roman letters $i, j, \ldots$ denote spatial indices, 1 through $d - 1$. In propagators the diagonal color factors are suppressed. The bare three-gluon vertex between gluons $A_\mu^a(P)$, $A_\nu^b(Q)$, and $A_\lambda^c(R)$ is

$$-igf^{abc}\Gamma^{\mu\nu\lambda}(P,Q,R) = -igf^{abc}\big((P-Q)^\lambda \delta^{\mu\nu} + \text{perm.}\big), \tag{3.1}$$

where $P + Q + R = 0$. We uniformly define all momenta to flow into a vertex. The bare four-gluon vertex, when traced over its last two color indices, is diagonal in its first two indices. We denote this component of the four-gluon vertex by

$$-g^2 N_c \delta^{ab}\Gamma^{\mu\nu\lambda\sigma}(P,Q,R,S) \equiv -g^2\delta^{ab}N_c(2\delta^{\mu\nu}\delta^{\lambda\sigma} - \delta^{\mu\lambda}\delta^{\nu\sigma} - \delta^{\mu\sigma}\delta^{\nu\lambda}), \tag{3.2}$$

with $P + Q + R + S = 0$. The generators of the adjoint representation are $(T^a)_{bc} = f^{bac}$. The color trace is $\mathrm{tr}(T^a T^b) = -N_c\delta^{ab}$.

The bare quark–gluon vertex for a gluon $A_\mu^a(R)$ coupled to a quark and antiquark with momenta P and Q is

$$gt^a\tilde{\Gamma}^\mu(P,Q;R) = gt^a\gamma^\mu. \tag{3.3}$$

The generators t^a of the fundamental representation obey $\mathrm{tr}(t^a t^b) = -\delta^{ab}/2$ and their Casimir is $C_f = (N_c^2 - 1)/(2N_c)$. Whether the color trace, tr, is that for the fundamental or the adjoint representation should be clear from the context.

3.1. THE COULOMB GAUGE

In this section we compute all hard thermal loops in the Coulomb gauge. With gauge-fixing term $(\partial^i A_i^a)^2/2\xi_C$, the bare propagator for the gauge field is

$$\Delta_{00}^C(K) = \frac{1}{k^2} + \xi_C\frac{(k^0)^2}{k^4}, \qquad \Delta_{0i}^C(K) = \xi_C\frac{k^0 k^i}{k^4}, \qquad \Delta_{ij}^C(K) = \Delta_{ij}^{tr}(K) + \xi_C\frac{\hat{k}^i\hat{k}^j}{k^2}. \tag{3.4}$$

Strict Coulomb gauge is $\xi_C = 0$, but we consider arbitrary values of ξ_C. The only

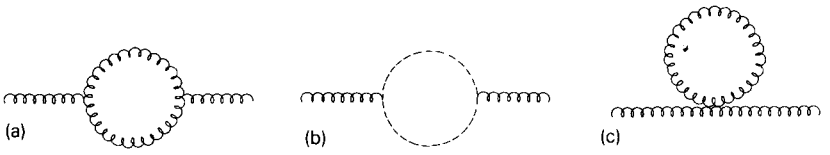

Fig. 3. One-loop diagrams which contribute to the gluon self-energy.

propagating modes are transverse gluons, with the propagator

$$\Delta_{ij}^{\rm tr}(K) = (\delta^{ij} - \hat{k}^i\hat{k}^j)\Delta(K)\,. \tag{3.5}$$

All of the other gluon modes, such as the timelike Coulomb gluon, Δ_{00}, are static. The Coulomb ghost is also static, with bare propagator $1/k^2$. It couples to spatial gluons through the vertex $-igf^{abc}p^i$, where p^i is the spatial momentum of the antighost leg.

To illustrate the analysis of a general amplitude, we compute the hard thermal loops in the gluon and quark self-energies. These were first calculated by Silin, Klimov, and Weldon [9–12]. Once we can calculate these efficiently, the extension to N-point functions at $N \geqslant 3$ is immediate.

The diagrams that contribute to the gluon self-energy at one-loop order are shown in fig. 3. The diagram with two three-gluon interactions, fig. 3a, contributes

$$\delta\Pi_{\rm 3g}^{\mu\nu}(P) \approx -\frac{g^2N_{\rm c}}{2}\,{\rm Tr}\,\Gamma^{\sigma\mu\lambda}(-P+K,P,-K)\Delta_{\lambda\lambda'}^{\rm C}(K)$$
$$\times\Gamma^{\lambda'\nu\sigma'}(-K,P,-P+K)\,\Delta_{\sigma'\sigma}^{\rm C}(P-K)\,. \tag{3.6}$$

The prefix δ is introduced to denote the hard thermal loop in an amplitude.

Many of the terms that appear in eq. (3.6) do not contribute to a hard thermal loop, and can be dropped at the outset. Since the loop momentum K is hard and the external momentum P is soft, the terms linear in P in the three-gluon vertices can be neglected in comparison to those linear in K. Thus the three-gluon vertex reduces to

$$\Gamma^{\sigma\mu\lambda}(-P+K,P,-K) \approx \Gamma^{\sigma\mu\lambda}(K,0,-K) = -2K^\mu\delta^{\sigma\lambda} + K^\sigma\delta^{\mu\lambda} + K^\lambda\delta^{\mu\sigma}\,. \tag{3.7}$$

The symbol " $\approx$ " is used here to denote an approximation that is valid for the hard thermal loop in an integral.

We concentrate on the term in eq. (3.6) that arises when both of the virtual gluons are transverse; it turns out that this contribution typifies the hard thermal loops for the N-point functions at $N \geqslant 3$. Several approximations can be made for transverse gluons in the Coulomb gauge. For soft P and hard K, the transverse propagator is proportional to a projection operator in $\boldsymbol{k}$:

$$\Delta_{ij}^{\rm tr}(P-K) = \left(\delta^{ij} - \frac{(\boldsymbol{p}-\boldsymbol{k})^i(\boldsymbol{p}-\boldsymbol{k})^j}{(\boldsymbol{p}-\boldsymbol{k})^2}\right)\Delta(P-K) \approx (\delta^{ij} - \hat{k}^i\hat{k}^j)\Delta(P-K)\,. \tag{3.8}$$

Consider what happens in eq. (3.6) when the three-gluon vertex of eq. (3.7) is sandwiched between two transverse propagators. As the propagators are transverse, the loop indices $\sigma, \lambda, \ldots$ must all be spatial: $\sigma = j$, $\lambda = i$, etc. Then any term in the three-gluon vertex which involves the loop indices, k^i or k^j, vanishes upon contraction with the transverse propagator. The only term which survives is from the first term in eq. (3.7), proportional to $-2K^\mu$:

$$\Delta_{ii'}^{\rm tr}(P-K)\Gamma^{i'\nu j'}(-K,0,K)\Delta_{j'j}^{\rm tr}(K) \approx -2K^\nu(\delta^{ij} - \hat{k}^i\hat{k}^j)\Delta(K)\Delta(P-K)\,. \tag{3.9}$$

Thus when a three-gluon vertex is sandwiched between two transverse gluon propagators, the projection operator in $\boldsymbol{k}$ survives unscathed. Consequently it is easy to contract the remaining vertex with eq. (3.9). As before any terms proportional to k^i or k^j vanish upon contraction with eq. (3.9), so the remaining vertex contributes $2K^\mu\delta^{ij}$. Contraction of the Kronecker delta δ^{ij} with the projection operator in eq. (3.9) gives an overall multiplicative factor of

$$\delta^{ij}(\delta^{ij} - \hat{k}^i\hat{k}^j) = d - 2\,. \tag{3.10}$$

The complete hard thermal loop in Π_{3g} is a sum of two terms,

$$\delta\Pi_{3g}^{\mu\nu}(P) \approx 2(d-2)g^2N_{\rm c}{\rm Tr}\,K^\mu K^\nu\Delta(K)\Delta(P-K) + g^2N_{\rm c}\,{\rm Tr}\big(\delta^{\mu i}\delta^{\nu j}\Delta_{ij}^{\rm tr}(K)\big)\,. \tag{3.11}$$

The first term is momentum dependent, proportional to $\mathscr{I}^{\mu\nu}(0,P)$. It arises just from the contribution of two transverse gluons, as discussed above. The second term, proportional to ${\rm Tr}\,\Delta^{\rm tr}(K)$, is a constant. It is only nonzero when the indices $\mu = \nu$ are spatial, and is due to the contribution of one transverse and one timelike gluon, Δ_{00}.

The Coulomb ghosts are static, so the ghost loop in fig. 3b cannot produce a hard thermal loop. The tadpole from the four-gluon vertex diagram of fig. 3c produces terms independent of the external momentum. The hard thermal loop, which comes from transverse gluons only, is

$$\delta\Pi^{\mu\nu}_{4g}(P) \approx -g^2 N_c \,\mathrm{Tr}\Big((d-2)\delta^{\mu\nu}\Delta(K) - \delta^{\mu i}\delta^{\nu j}\Delta^{tr}_{ij}(K)\Big). \tag{3.12}$$

The second term in eq. (3.12) cancels identically against the constant term in eq. (3.11). Adding eqs. (3.11) and (3.12) together, we find that the contribution of virtual gluons to the hard thermal loop in the gluon self-energy is

$$\delta\Pi^{\mu\nu}_{3g+4g+gh}(P) \approx 2(d-2)g^2 N_c \,\mathrm{Tr}\big(K^\mu K^\nu \Delta(K)\Delta(P-K) - \tfrac{1}{2}\delta^{\mu\nu}\Delta(K)\big). \tag{3.13}$$

This result is independent of the Coulomb gauge-fixing parameter ξ_C.

Notice that it is much simpler to compute just the momentum-dependent part of $\delta\Pi^{\mu\nu}$ in eq. (3.13). This is due solely to the contribution of two transverse gluons, for which the approximations of eqs. (3.7)–(3.9) apply. The constant term in $\delta\Pi^{\mu\nu}$ is more involved, for then the static modes, through the constant term in eq. (3.11), and four-gluon vertices, eq. (3.12), contribute. Fortunately, these complications are special to the constant term in the gluon self-energy, and do not enter into the hard thermal loops of N-gluons when $N \geqslant 3$.

We remark that the constant term in the gluon self-energy has a direct physical interpretation. Since it is a constant, its value can be determined at any momentum. The most convenient choice is at zero momentum, where the behavior of the gluon self-energy is a familiar story [1]. For instance, choosing $p^0 = 0$ and then setting $p \to 0$, the only nonzero component of $\Pi^{\mu\nu}$ is $\Pi^{00} = m_{el}^2 \sim g^2 T^2$. To this order the electric mass m_{el} is the inverse screening length for static electric fields, and is a physical quantity. In subsects. 3.2 and 3.3 we show that in covariant gauges the constant term in the gluon self-energy arises in a way very different from in Coulomb gauge. Yet since m_{el} is a physical quantity, and so gauge invariant, we can rest assured that in the end, the sum of all such constant terms is bound to be the same.

The contribution of the quark loop to the gluon self-energy is

$$\delta\Pi^{\mu\nu}_{q}(P) \approx \frac{g^2 N_f}{2}\mathrm{Tr}\big(\gamma^\mu \Delta_f(K)\gamma^\nu \Delta_f(K-P)\big), \tag{3.14}$$

where the quark propagator Δ_f is given in eq. (2.6), and there is an implied trace over the Dirac indices. Like the three-gluon vertex in eq. (3.7), terms linear in $\not{P}$ in the numerator of the second quark propagator can be dropped:

$$\Delta_f(P-K) \approx -i\not{K}\tilde{\Delta}(P-K). \tag{3.15}$$

This makes the trace over Dirac indices simple, and eq. (3.14) reduces to

$$\delta\Pi_{\rm q}^{\mu\nu}(P) \approx -2^{d/2}N_{\rm f}g^2\,{\rm Tr}\Big(K^\mu K^\nu\tilde{\Delta}(K)\tilde{\Delta}(P-K) - \tfrac{1}{2}\delta^{\mu\nu}\tilde{\Delta}(K)\Big), \quad (3.16)$$

where the factor of $2^{d/2}$ is from the dimensionality of the Dirac matrices.

The hard thermal loops in eqs. (3.13) and (3.16) are given as integrals which can be rewritten in terms of the functions $\mathscr{I}$ and $\tilde{\mathscr{I}}$ of sect. 2. The contribution of the quark loop involves the function $\tilde{\mathscr{I}}$, but the identity of eq. (2.36) can be used to exchange $\tilde{\mathscr{I}}$ for $\mathscr{I}$. Setting $d=4$, the complete hard thermal loop in the gluon self-energy is

$$\delta\Pi^{\mu\nu}(P) = 4g^2\big(N_{\rm c}+\tfrac{1}{2}N_{\rm f}\big)\big(\mathscr{I}^{\mu\nu}(0,P) - \tfrac{1}{2}\delta^{\mu\nu}\mathscr{I}(0)\big). \quad (3.17)$$

This is the self-energy calculated by Silin, Klimov, Weldon and others [5, 9–12], expressed in our compact notation.

As a second example, consider the quark self-energy. To one-loop order,

$$\delta\Sigma(P) \approx g^2C_{\rm f}\,{\rm Tr}\big(\gamma^\mu\Delta_{\rm f}(P-K)\gamma^\nu\Delta_{\mu\nu}^{\rm C}(K)\big). \quad (3.18)$$

Using eq. (3.15), we drop the soft $\not{P}$ in the numerator of the quark propagator. The numerator in the trace is proportional to

$$\gamma^i\not{K}\gamma^j(\delta^{ij}-\hat{k}^i\hat{k}^j) = -(d-2)\not{K}. \quad (3.19)$$

Only transverse gluons contribute to the hard thermal loop in Σ, and give

$$\delta\Sigma(P) \approx -i(d-2)g^2C_{\rm f}\,{\rm Tr}\,\not{K}\Delta(K)\tilde{\Delta}(P-K). \quad (3.20)$$

Setting $d=4$, and expressing it in terms of the $\mathscr{I}$ function defined in sect. 2, we find that

$$\delta\Sigma(P) = -2ig^2C_{\rm f}\gamma^\mu\mathscr{I}^\mu(0;P). \quad (3.21)$$

This is the quark self-energy calculated by Klimov and Weldon [11, 12].

It is surprisingly easy to generalize these two examples to calculate all hard thermal loops. This is because we can make two approximations for the N-point functions at $N\geqslant 3$ which cannot be made for the constant term in the gluon self-energy. The first approximation is that only transverse gluons contribute. From the power counting rules of sect. 2, each propagator for a transverse mode is of order $1/PT\sim 1/gT^2$ at soft P. In contrast, the propagator for any static mode is of order $1/k^2\sim 1/T^2$ at hard k. Thus the substitution of a static for a transverse mode reduces the diagram by a power of g.

The second approximation is that any diagram involving a four-gluon vertex can be neglected. Suppose that in a one-loop diagram, such as fig. 1a, two adjacent three-gluon vertices, plus the propagator connecting them, are replaced by a four-gluon vertex. By the power counting rules, the two adjacent three-gluon vertices each contribute g for the coupling constant and $K \sim T$, while the propagator connecting them gives $1/gT^2$; altogether this is of order $(gT)^2/(gT^2) = g$. In contrast, the four-gluon vertex is of order g^2. Thus diagrams with one four-gluon vertex are at most g times a hard thermal loop.

These approximations do not apply to the constant term in the gluon self-energy because this term only involves an integral over one propagator, such as $\mathrm{Tr}\,\Delta(K)$. Only for integrals with two or more propagators is there a suppression factor of P/T from the cancelling statistical distribution functions between particles of the same statistics.

Using these approximations, we see that the only contribution to the N-gluon amplitude is from the gluon loop of fig. 1, when all of the virtual gluons inside the loop are transverse. Using eq. (3.8), each of the N transverse propagators contributes $\Delta(P-K)$ times a projection operator. The N three-gluon vertices are approximately those of eq. (3.7). When sandwiched between two transverse gluons, each vertex simplifies as in eq. (3.9), to contribute a factor of the coupling g times $2K^\mu$. The projection operator in $\boldsymbol{k}$ runs around the loop until it contracts upon itself to give $d-2$, eq. (3.10). The resulting integral is that of eq. (2.27), which through the $\mathscr{J}$ function has a hard thermal loop. Summing over all diagrams of the form in fig. 1a, the result is

$$\delta\Gamma_{\mathrm{g}}^N = \frac{(d-2)}{2}(-2ig)^N \sum_{\mathrm{perm}} \mathrm{tr}(T^{a_1}\ldots T^{a_N})\mathscr{J}^{\mu_1\cdots\mu_N}(0,P_1,\ldots,P_{N-1}), \quad N>2. \tag{3.22}$$

We have ordered the external gluon lines so that the lth line is for the gluon $A_{\mu_l}^{a_l}(P_l - P_{l-1})$, defining $P_0 = P_N = 0$. The particular term displayed in eq. (3.22) occurs when the external legs are ordered consecutively, but the sum runs over all noncyclic permutations of the external lines. Notice that when $N=2$, the overall coefficient, $2(d-2)$, agrees with that found for the two-point function in eq. (3.13). Eq. (3.22) represents the complete contribution from virtual gluons and ghosts to the N-gluon hard thermal loop for $N \geqslant 3$; all other terms are smaller by at least one power of g.

The quark loop in fig. 1b also contributes to the hard thermal part of the N-gluon amplitude. In the quark loop, we can use eq. (3.15) to write

$$\Delta_{\mathrm{f}}(P-K)\gamma^\mu\Delta_{\mathrm{f}}(P'-K) \approx -(\not{K}\gamma^\mu\not{K})\tilde{\Delta}(P-K)\tilde{\Delta}(P'-K). \tag{3.23}$$

In hard thermal loops we can take

$$\not{K}\gamma^{\mu}\not{K} = 2K^{\mu}\not{K} - K^2\gamma^{\mu} \approx 2K^{\mu}\not{K}. \tag{3.24}$$

The term $K^2\gamma^{\mu}$ is dropped because the K^2 cancels $\tilde{\Delta}(K)$: the resulting integral, with two less powers of K and one less $\tilde{\Delta}$, is not a hard thermal loop when $N \geqslant 3$. Applying the approximations of eqs. (3.23) and (3.24) at every vertex, the Dirac trace is trivial. Each of the N vertices contributes $2K^{\mu}$, while each virtual fermion line adds $\tilde{\Delta}(P-K)$. The integral which results is the function $\tilde{\mathscr{J}}$ defined in eq. (2.28). Summing over all diagrams of the form shown in fig. 1b, quarks contribute to the hard thermal loop in the N-gluon amplitude as

$$\delta\Gamma_{\rm q}^{N} = -2^{d/2-1}N_{\rm f}(-2ig)^{N}\sum_{\rm perm}\mathrm{tr}(t^{a_1}\ldots t^{a_N})\tilde{\mathscr{J}}^{\mu_1\cdots\mu_N}(0,P_1,\ldots,P_{N-1}), \quad N>2. \tag{3.25}$$

Compare the overall coefficient, $-2^{d/2-1}N_{\rm f}$, with the $(d-2)/2$ from the gluon loop, eq. (3.22). The $d-2$ is just the number of transverse gluons. For the quark loop, there is $N_{\rm f}$ from the number of flavors, $2^{d/2}$ from the Dirac trace, and an overall minus sign from the Fermi statistics. Eq. (2.36) can be used to change the $\tilde{\mathscr{J}}$ function in eq. (3.25) to an $\mathscr{J}$ function; this changes the overall coefficient to $+2^{d/2-2}N_{\rm f}$.

In Coulomb gauge the hard thermal loop in the amplitude between a quark pair and $N-2$ gluons is generated by the diagrams of fig. 2. The approximations discussed for the N-gluon amplitude apply; for instance, in fig. 2 all of the virtual gluons are transverse. This hard thermal loop is most transparent when written in a functional form, which is given below in eq. (3.38).

Before proceeding to derive generating functionals for hard thermal loops, we give explicit expressions for the hard thermal loops in the three- and four-point functions. For the three-gluon amplitude, the sum of the hard thermal loops in eqs. (3.22) and (3.25) is

$$\delta\Gamma^{\mu\nu\lambda}(P,Q,R) = -8g^2\left(N_{\rm c}+\tfrac{1}{2}N_{\rm f}\right)\mathscr{J}^{\mu\nu\lambda}(0,P,-Q), \tag{3.26}$$

where $P+Q+R=0$. Note that the coefficient $N_{\rm c}+N_{\rm f}/2$ is the same as in the gluon self-energy, eq. (3.17). The hard thermal loop in the quark–gluon vertex is

$$\delta\tilde{\Gamma}^{\mu}(P,Q;R) = -4g^2C_{\rm f}\gamma^{\nu}\mathscr{J}^{\mu\nu}(0;P,-Q). \tag{3.27}$$

It is surprising to find that the hard thermal loop in the vertex is proportional to the Casimir $C_{\rm f}$, as found for the quark self-energy in eq. (3.21). The vertex correction in eq. (3.27) comes from two distinct diagrams, both of which are of the form shown in fig. 2. The first diagram is common to QED, but the second involves

the nonabelian three-gluon coupling, and so is special to QCD. In general these two diagrams are not simply related to each other, but their hard thermal loops are related by the conjugation identity of eq. (2.38), so that they combine to give a result which is proportional to C_f.

For the four-point functions, we give the hard thermal loops for amplitudes which are summed in the color indices for two of the gluon legs. These are the only amplitudes that are required for the calculations of self-energies in sect. 4. At tree level the four-gluon amplitude is given in eq. (3.2). The hard thermal loop for this amplitude is

$$\delta\Gamma^{\mu\nu\lambda\sigma}(P,Q,R,S) = -32g^2\frac{1}{N_c}\left(\left(N_c^2+\frac{C_f N_f}{2}\right)\right.$$
$$\times\left(\mathscr{J}^{\mu\nu\lambda\sigma}(0,P,P+Q,-R)+\mathscr{J}^{\mu\nu\lambda\sigma}(0,P,P+Q,-S)\right)$$
$$\left.+\frac{1}{2}\left(N_c^2-\frac{N_f}{2N_c}\right)\mathscr{J}^{\mu\nu\lambda\sigma}(0,P,P+R,-S)\right), \tag{3.28}$$

with $P+Q+R+S=0$.

At tree level there is no coupling between a quark pair and two gluons. Such an amplitude is induced at one-loop order, through the diagrams of fig. 2. Three distinct diagrams contribute to the hard thermal loop. Summing over the color indices of the two gluons, the amplitude equals $-ig^2C_f\delta\tilde{\Gamma}^{\mu\nu}$, where

$$\delta\tilde{\Gamma}^{\mu\nu}(P,Q;R,S)$$
$$= -8g^2\gamma^\lambda\left[(C_f+N_c)\left(\mathscr{J}^{\mu\nu\lambda}(0,-R,P+Q;P)+\mathscr{J}^{\mu\nu\lambda}(0,-S,P+Q;P)\right)\right.$$
$$\left.+\tfrac{1}{2}N_c\left(\mathscr{J}^{\mu\nu\lambda}(0,-S;P,P+R)+\mathscr{J}^{\mu\nu\lambda}(0,-R;P,P+S)\right)\right]. \tag{3.29}$$

Note that the bare amplitude vanishes: $\tilde{\Gamma}^{\mu\nu}=0$.

The Ward identities satisfied by hard thermal loops follow from eqs. (2.40) and (2.41). Because these relations are so simple, so are the Ward identities. For the gluon self-energy in (3.17), eq. (2.41) shows that it is transverse,

$$P^\mu\delta\Pi^{\mu\nu}(P)=0. \tag{3.30}$$

The other Ward identities can be read off from eq. (2.40). For the three-point functions, they are

$$R^\lambda\delta\Gamma^{\mu\nu\lambda}(P,Q,R)=\delta\Pi^{\mu\nu}(P)-\delta\Pi^{\mu\nu}(Q), \tag{3.31}$$

$$R^\mu\delta\tilde{\Gamma}^{\mu}(P,Q;R)=i\delta\Sigma(P)+i\delta\Sigma(Q). \tag{3.32}$$

After tracing over the color indices of two gluon legs, the four-point functions have a trivial color structure, and obey Ward identities similar to those for the three-point functions:

$$S^{\sigma}\delta\Gamma^{\mu\nu\lambda\sigma}(P,Q,R,S) = \delta\Gamma^{\mu\nu\lambda}(P+S,Q,R) - \delta\Gamma^{\mu\nu\lambda}(P,Q+S,R)\,, \quad (3.33)$$

$$S^{\nu}\delta\tilde{\Gamma}^{\mu\nu}(P,Q;R,S) = \delta\tilde{\Gamma}^{\mu}(P+S,Q;R) - \delta\tilde{\Gamma}^{\mu}(P,Q+S;R)\,. \quad (3.34)$$

These Ward identities are used in sect. 4 to prove the gauge invariance of two-point $\mathscr{S}$-matrix elements.

We conclude this subsection by deriving generating functionals which succinctly summarize all hard thermal loops. For amplitudes between N-gluons, eqs. (3.22) and (3.25) can be written as a functional $\delta S[A]$:

$$\begin{aligned}\delta S[A] = \sum_{N=2}^{\infty} \delta\Gamma^{N}\frac{A^{N}}{N!} \approx {} & \left((d-2)N_{\mathrm{c}} + 2^{d/2-1}N_{\mathrm{f}}\right)g^{2}T^{2}\int \mathrm{d}^{4}x\,(A_{\mu}^{a})^{2} \\ & + \left(\frac{d-2}{2}\right)\int \mathrm{d}^{4}x\,\mathrm{Tr}\,\mathrm{tr}\log\left((-i\partial^{\mu}-K^{\mu})^{2} - 2igT^{a}A_{\mu}^{a}(x)K^{\mu}\right) \\ & + \left(2^{d/2-2}N_{\mathrm{f}}\right)\int \mathrm{d}^{4}x\,\mathrm{Tr}\,\mathrm{tr}\log\left((-i\partial^{\mu}-K^{\mu})^{2} - 2igt^{a}A_{\mu}^{a}(x)K^{\mu}\right).\end{aligned} \quad (3.35)$$

In this expression A_{μ}^{a} is assumed to be an arbitrary external gauge field with soft momenta. The term proportional to $(A_{\mu}^{a})^{2}$ arises from the constant term in the gluon self-energy, eq. (3.17). The logarithm proportional to $d-2$ sums the contributions of all gluons loops in fig. 1a, eq. (3.22); the logarithm proportional to N_{f} sums the fermion loops in fig. 1b, eq. (3.25). In the logarithms the factors of the loop momenta K are explicit, while the derivatives ∂ act just on the soft gauge fields. In eq. (3.35) A_{μ}^{a} is written in coordinate space; as each logarithm is expanded in powers of $A_{\mu}^{a}(x)$, transformation from coordinate to momentum space gives

$$\frac{1}{(-i\partial^{\nu}-K^{\nu})^{2}}A_{\mu}^{a}(x)K^{\mu}\frac{1}{(-i\partial^{\nu}-K^{\nu})^{2}} \to \Delta(P-K)K^{\mu}\Delta(P'-K)A_{\mu}^{a}(P-P')\,. \quad (3.36)$$

Eq. (3.35) is so simple because expansion of the logarithms automatically incorporates the sum over permutations of the external lines in eqs. (3.22) and (3.25).

The generating functional $\delta S[A]$ can be derived more directly. Suppose the quark and gluon fields are divided into those with hard and those with soft

momenta. Integration over the hard fields produces an effective action which is a functional of the soft, background field A_μ^a. At one-loop order, the contribution of hard virtual gluons to $\delta S[A]$ is related to the gluon propagator in a background gluon field,

$$\delta S_g[A] \approx -\tfrac{1}{2} V \,\mathrm{Tr}\,\mathrm{tr}\log\left(-D^2\delta^{\mu\nu} + D^\mu D^\nu + 2gF^{\mu\nu} - \frac{1}{\xi_C}\partial^i\partial^j\delta^{\mu i}\delta^{\nu j}\right). \quad (3.37)$$

$D_\mu = \partial_\mu - gT^a A_\mu^a$ is the covariant derivative for an adjoint field, etc. The approximations made previously diagram by diagram can be made directly in eq. (3.37). Except for the two-point function, diagrams with four-gluon interactions do not contribute to hard thermal loops; this corresponds to dropping terms proportional to $(A_\mu^a)^2$ in eq. (3.37). Similarly, since the field strength tensor $F^{\mu\nu}$ is that for the soft background field, it is proportional to a soft momentum, and so negligible. In this way the inverse gluon propagator in eq. (3.37) reduces to the inverse propagator of an adjoint scalar, which is the argument of the logarithm in the term proportional to $d-2$ in eq. (3.35). Likewise, in the term proportional to N_f, the operator is the approximate form for the inverse quark propagator in a soft, background gluon field.

A generating functional can also be derived for the hard thermal loops between a quark pair and any number of gluons:

$$\begin{aligned}\delta\tilde{S}[\bar{\psi},\psi,A] &= \sum_{N=2}^{\infty}\delta\tilde{\Gamma}^N\frac{\bar{\psi}A^{N-2}\psi}{(N-2)!}\\ &\approx i(d-2)g^2\int \mathrm{d}^4x\,\mathrm{Tr}\,\bar{\psi}\not{K}t^a\frac{1}{(-i\partial^\mu+K^\mu)^2+2igt^cA_\mu^c(x)K^\mu}t^b\psi\\ &\quad\times\left(\frac{1}{(-i\partial^\mu-K^\mu)^2-2igT^dA_\mu^d(x)K^\mu}\right)_{ab}. \end{aligned} \quad (3.38)$$

In this expression the momentum operator $-i\partial_\mu$ acts on both the gluon fields $A_\mu(x)$ and on the quark field $\psi(x)$. Under the approximations that produce hard thermal loops, this functional is the quark self-energy to one-loop order, in the presence of a soft, background gluon field.

3.2. THE FEYNMAN GAUGE

In this subsection we show that the hard thermal loops in the Feynman gauge are identical to those in the Coulomb gauge. With a gauge-fixing term

$(\partial^\mu A^a_\mu)^2/(2(1-\xi))$, the bare gauge propagator is

$$\Delta_{\mu\nu}(K) = \delta^{\mu\nu}\Delta(K) - \xi K^\mu K^\nu \Delta^2(K) = \Delta^{\rm F}_{\mu\nu}(K) - \xi \Delta^\xi_{\mu\nu}(K) . \qquad (3.39)$$

In this subsection we restrict ourselves to the Feynman gauge, which is the choice $\xi = 0$. The ghosts in covariant gauge propagate, with the bare propagator $\Delta(K)$. The vertex between a gluon $A^a_\mu(P)$, a ghost $\eta^b(Q)$, and an antighost $\bar\eta^c(R)$ is $igf^{abc}R^\mu$. As discussed in sect. 2, amplitudes with ghosts as external lines do not have hard thermal loops. On the other hand, in covariant gauges virtual ghosts do propagate, and contribute to the hard thermal loops of N-gluon amplitudes.

As before we start with the example of the gluon self-energy. In eq. (3.6), Coulomb propagators are replaced by those in Feynman gauge, $\Delta^{\rm F}$. Each of the three-gluon vertices can be approximated by the sum of three terms, as in eq. (3.7). In the Coulomb gauge, only one term survives when this vertex is sandwiched between two transverse propagators, eq. (3.9). In the Feynman gauge, however, all three terms survive and contribute to hard thermal loops. We organize the calculation of the hard thermal loop in a way which generalizes easily to the N-gluon amplitude. Consider the product of two three-gluon vertices, as in eq. (3.6), tied together by a Feynman propagator. For hard K, this reduces to

$$\begin{aligned}\Gamma^{\sigma\mu\lambda}(K,0,-K)\Delta^{\rm F}_{\lambda\lambda'}(K)\Gamma^{\lambda'\nu\sigma'}(-K,0,K) \\ = -(4K^\mu K^\nu \delta^{\sigma\sigma'} - 2K^\sigma K^\nu \delta^{\mu\sigma'} - 2K^\mu K^{\sigma'}\delta^{\nu\sigma} \\ - K^\mu K^\sigma \delta^{\nu\sigma'} - K^{\sigma'}K^\nu\delta^{\mu\sigma} + K^2\delta^{\mu\sigma}\delta^{\nu\sigma'} + K^\sigma K^{\sigma'}\delta^{\mu\nu})\Delta(K) . \qquad (3.40)\end{aligned}$$

Multiplying eq. (3.40) by the remaining Feynman propagator $\Delta^{\rm F}_{\sigma'\sigma}(P-K)$, we find that in the Feynman gauge the hard thermal loop in fig. 3a is

$$\delta\Pi^{\mu\nu}_{\rm 3g}(P) \approx \frac{g^2 N_{\rm c}}{2} {\rm Tr}\big((4d-6)K^\mu K^\nu + 2\delta^{\mu\nu}K^2\big)\Delta(K)\Delta(P-K) . \qquad (3.41)$$

In the Feynman gauge there are also hard thermal loops from the virtual ghosts of fig. 3b and from the tadpole diagram of fig. 3c. The ghost loop is easy to evaluate, because the dependence on the soft external momenta in the ghost–gluon vertices can be dropped, so that the two vertices are proportional to K^μ and K^ν. The sum of the contributions to the hard thermal loop from figs. 3a–c is

$$\begin{aligned}\delta\Pi^{\mu\nu}_{\rm 3g+4g+gh}(P) \approx \frac{g^2 N_{\rm c}}{2} {\rm Tr}\big(((4d-6)-2)K^\mu K^\nu \Delta(K)\Delta(P-K) \\ + (2-2(d-1))\delta^{\mu\nu}\Delta(K)\big) . \qquad (3.42)\end{aligned}$$

In the momentum-dependent term, the piece proportional to $4d-6$ is from eq. (3.41), while that proportional to -2, is from the ghost loop of fig. 3b. The constant term also receives two contributions: the 2 is from eq. (3.41), the $-2(d-1)$ is from the tadpole diagram of fig. 3c. Eq. (3.42) is equal to the corresponding result in the Coulomb gauge, eq. (3.13). Since there is no change in the contribution from the quark loop, eq. (3.16), we conclude that $\delta\Pi^{\mu\nu}$ is the same in the Coulomb and Feynman gauges.

Our second example is the quark self-energy. In eq. (3.18) we substitute the Feynman for the Coulomb propagator. The numerator inside the trace is proportional to

$$\gamma^{\mu}\not{K}\gamma^{\mu} = -(d-2)\not{K}. \tag{3.43}$$

Since the right-hand side here equals that of eq. (3.19), this hard thermal loop is the same in the Feynman gauge as in the Coulomb gauge, eq. (3.20).

With these examples in hand we turn to the N-point functions at $N \geqslant 3$. The calculation of the hard thermal loop in the N-gluon amplitudes is a straightforward generalization of that for the momentum-dependent term in the gluon self-energy. The only diagrams which contribute at $N \geqslant 3$ are those of fig. 1a, from a gluon loop, plus the analogous diagram from a ghost loop; any diagrams with four-gluon vertices do not contain hard thermal loops. In fig. 1a, the three-gluon vertices can be approximated as in eq. (3.7). Sewing two such vertices together with a Feynman propagator gives eq. (3.40). If N vertices are sewed together with $N-1$ Feynman propagators, the numerator reduces to

$$\begin{aligned}\not{\gamma}^{\sigma_1\mu_1\ldots\mu_N\sigma_{N+1}} &= \Gamma^{\sigma_1\mu_1\sigma_2}(-K,0,K)\,\Gamma^{\sigma_2\mu_2\sigma_3}(-K,0,K)\ldots\Gamma^{\sigma_N\mu_N\sigma_{N+1}}(-K,0,K)\\ &\approx 2^N K^{\mu_1}K^{\mu_2}\ldots K^{\mu_N}\delta^{\sigma_1\sigma_{N+1}} - \sum_{l=1}^{N} 2^{N-l}\big(K^{\mu_1}\ldots K^{\mu_{l-1}}K^{\sigma_1}K^{\mu_{l+1}}\\ &\quad\ldots K^{\mu_N}\delta^{\mu_l\sigma_{N+1}} + K^{\mu_1}\ldots K^{\mu_{N-l}}K^{\sigma_{N+1}}K^{\mu_{N+2-l}}\ldots K^{\mu_N}\delta^{\mu_{N+1-l}\sigma_1}\big).\end{aligned} \tag{3.44}$$

In this expression the μ indices refer to the external gluons, and the σ indices to the virtual gluons inside the loop. The virtual gluon indices σ_1 and σ_{N+1}, at each end of the string of N three-gluon vertices, are free. The result in eq. (3.44) is obtained by making approximations which are valid only for hard thermal loops. By the identity of eq. (2.33), when $N \geqslant 3$ all terms proportional to K^2, or to a Kronecker delta between two external indices, such as $\delta^{\mu_1\mu_2}$, can be dropped. With the neglect of such terms, eq. (3.44) can be proved inductively.

With eq. (3.44) in hand, it is direct to show that the hard thermal loops for an N-gluon amplitude in the Feynman gauge equal those in the Coulomb gauge. To obtain the numerator of the N-gluon amplitude, eq. (3.44) is contracted with $\delta^{\sigma_1\sigma_{N+1}}$ from the remaining Feynman propagator in the gluon loop. Each term is

proportional to $K^{\mu_1} \ldots K^{\mu_N}$, which is the usual numerator in a hard thermal loop, eq. (2.27). The first term in eq. (3.44) is proportional to $\delta^{\sigma_1 \sigma_{N+1}}$, and produces a factor of d; relative to this, every other term gives a 1. Thus the numerator of the amplitude is proportional to

$$\delta^{\sigma_1 \sigma_{N+1}} \not{\mathscr{V}}^{\sigma_1 \mu_1 \cdots \mu_N \sigma_{N+1}} = \mathscr{C}_{\mathrm{g}}^{N} K^{\mu_1} \ldots K^{\mu_N}, \tag{3.45}$$

where

$$\mathscr{C}_{\mathrm{g}}^{N} = 2^N d - \sum_{l=1}^{N} 2^l = 2^N d - 2^{N+1} + 2. \tag{3.46}$$

For $N = 2$, this coefficient is $4d - 6$, which agrees with the momentum-dependent term in eq. (3.41). The contribution of the ghost loop to the N-gluon amplitude is of the same form as the gluon loop: with the normalization of eq. (3.45), its contribution is $\mathscr{C}_{\mathrm{gh}}^{N} = -2$. The $(-)$ sign is from ghost statistics, the 2 from the sum of loops oriented in opposite directions. Thus in Feynman gauge the sum of the gluon and ghost loops has an overall coefficient

$$\mathscr{C}_{\mathrm{g}}^{N} + \mathscr{C}_{\mathrm{gh}}^{N} = 2^N (d - 2). \tag{3.47}$$

Comparison with eq. (3.22) shows that this equals the coefficient found before in the Coulomb gauge, and demonstrates that for N-gluons the hard thermal loops are the same in the two gauges. By similar means, one can show that the hard thermal loops for the amplitude between a quark pair and $N - 2$ gluons agree in both gauges.

3.3. COVARIANT GAUGES

In this subsection we show that in an arbitrary covariant gauge, the hard thermal loops of N-point functions are independent of the gauge parameter ξ. Klimov and Weldon first showed that the hard thermal loops in the self-energies are independent of ξ [11]. It is extraordinary to find that this gauge independence extends to *all* hard thermal loops, for the external legs do not have to be on the mass-shell; they just have to be soft. This property is special to leading order: relative to the tree amplitude, corrections of order g are in general gauge dependent off the mass-shell.

To appreciate the complications which arise in a general covariant gauge, start with a diagram which has a hard thermal loop in the Feynman gauge, such as in figs. 1a or 2. For one virtual gluon leg in the diagram, substitute the gauge-dependent piece of the propagator, $-\xi \Delta_{\mu\nu}^{\xi}(K)$ in eq. (3.39), for the Feynman propagator. This substitution adds an extra factor of $K^{\mu} K^{\nu} \Delta(K)$ to the integral. Following the power counting rules of sect. 2, each K^{μ} is proportional to T, and the propagator to $1/PT$, so this substitution produces terms which change the integral

by an overall factor of $T^2/PT \sim 1/g$ for soft P. Thus in individual diagrams, terms proportional to ξ^m can be $1/g^m$ times hard thermal loops.

Nevertheless, we prove that when all diagrams which contribute to a given N-point amplitude are added together, the dependence upon ξ cancels identically. Our proof proceeds in two steps. First we use the Ward identities for the bare propagators and vertices to show that diagram by diagram, all terms which are powers of $1/g$ times a hard thermal loop cancel. The terms which remain are ξ-dependent hard thermal loops. These arise both from diagrams which have hard thermal loops in the Feynman gauge, and from diagrams with four-gluon interactions, which do *not* have hard thermal loops in the Feynman gauge. We show that the sum of these ξ-dependent hard thermal loops vanishes in any amplitude. Our proof is inductive, using the simple form for the Ward identities satisfied by hard thermal loops.

As in previous sections we begin with the examples of the gluon and quark self-energies. Klimov and Weldon demonstrated that the hard thermal loops in these amplitudes are independent of ξ by direct calculation. We take a different approach, which directly generalizes to the higher N-point functions.

Consider the contribution to the gluon self-energy from the diagram of fig. 3a. Substituting the ξ-dependent gluon propagators of eq. (3.39) for the Coulomb propagators in eq. (3.6), we find that the ξ-dependent part of the hard thermal loop in fig. 3a is given by

$$\delta\Pi^{\mu\nu}_{\xi,3g}(P) \approx -\frac{g^2 N_c}{2}\,\mathrm{Tr}\,\Gamma^{\sigma\mu\lambda}(-P+K,P,-K)\big(2\xi\Delta^{F}_{\lambda\lambda'}(K)+\xi^2\Delta^{\xi}_{\lambda\lambda'}(K)\big)$$

$$\times\Gamma^{\lambda'\nu\sigma'}(-K,P,-P+K)\Delta^{\xi}_{\sigma'\sigma}(P-K)\,. \tag{3.48}$$

The ξ dependence arises from the part of the gluon propagator proportional to Δ^{ξ}, which can be inserted on either one or on both legs of the diagram. The single insertions give the same result, so we assume that the insertion is on the leg with momentum $P-K$, and multiply by two.

The rules for simplifying diagrams must be modified when dealing with ξ-dependent terms. As noted above, for terms linear in ξ, the integrals contain terms which are $1/g$ times a hard thermal loop. Consequently, to keep all hard thermal loops, it is necessary to retain terms with one power of the soft momentum P. In general, for terms proportional to ξ^m, terms up to order P^m must be included.

Eq. (3.48) can be simplified most directly by using the Ward identities. We introduce the transverse inverse propagator

$$\Delta^{-1}_{\mu\nu}(K) = \delta^{\mu\nu}K^2 - K^\mu K^\nu\,. \tag{3.49}$$

Our notation is unconventional, for Δ^{-1} is not the full inverse propagator: it

excludes the terms for gauge fixing, and is therefore not invertible. The notation is convenient, however, because it is Δ^{-1} that enters into the Ward identity for the bare three-gluon vertex:

$$(K-P)^{\sigma}\Gamma^{\sigma\mu\lambda}(-P+K,P,-K) = -\Delta^{-1}_{\mu\lambda}(P)+\Delta^{-1}_{\mu\lambda}(K)\,. \tag{3.50}$$

The transverse inverse propagator is proportional to a projection operator, and so satisfies some simple identities. When contracted with the covariant propagator,

$$\Delta^{-1}_{\mu\lambda}(K)\Delta^{\lambda\nu}(K) = \Delta^{-1}_{\mu\nu}(K)\Delta(K)\,, \tag{3.51}$$

because the transverse inverse propagator annihilates the gauge-dependent term,

$$\Delta^{-1}_{\mu\lambda}(K)\Delta^{\xi}_{\lambda\nu}(K) = 0\,. \tag{3.52}$$

Also, the product of two Δ^{-1} is

$$\Delta^{-1}_{\mu\lambda}(K)\Delta^{-1}_{\lambda\nu}(K) = K^2\Delta^{-1}_{\mu\nu}(K)\,. \tag{3.53}$$

From the form of eq. (3.48), it is evident why the bare Ward identity is of help. The term $\Delta^{\xi}_{\sigma\sigma'}(P-K)$ is proportional to $(P-K)^{\sigma}(P-K)^{\sigma'}$. Each of the $(P-K)$'s is contracted with a three-gluon vertex, and can be simplified using eq. (3.50). The result is

$$\begin{aligned}\delta\Pi^{\mu\nu}_{\xi,3g} \approx & -\tfrac{1}{2}g^2N_c\,\mathrm{Tr}\,\Delta^2(P-K)\big(\Delta^{-1}_{\mu\lambda}(K)-\Delta^{-1}_{\mu\lambda}(P)\big)\\ & \times\big(2\xi\Delta^{F}_{\lambda\lambda'}(K)+\xi^2\Delta^{\xi}_{\lambda\lambda'}(K)\big)\big(\Delta^{-1}_{\lambda'\nu}(K)-\Delta^{-1}_{\lambda'\nu}(P)\big)\,.\end{aligned} \tag{3.54}$$

It is easy to see that the term proportional to ξ^2 does not contain a hard thermal loop. The factors of $\Delta^{-1}(K)$ can be dropped because of eq. (3.52). The remaining term involves two factors of $\Delta^{-1}(P)$, so it is of order P^4; this integral is at most g^2 times a hard thermal loop, and so is negligible. For the term proportional to ξ, as the integral is no more than $1/g$ times a hard thermal loop, factors of $\Delta^{-1}(P)\sim P^2$ can be dropped. The remaining term can be simplified by using eqs. (3.51) and (3.53). The final result is

$$\delta\Pi^{\mu\nu}_{\xi,3g} \approx -\xi g^2N_c\,\mathrm{Tr}\big(\Delta^2(P-K)\Delta^{-1}_{\mu\nu}(K)\big)\,. \tag{3.55}$$

Shifting the integration variable, we find that the hard thermal loop is a constant, independent of the momentum P. It cancels identically against a contribution from the four-gluon vertex diagram of fig. 3c. The ghost loop of fig. 3b and the quark loop are independent of ξ, so this establishes that the hard thermal loop in the

gluon self-energy is independent of ξ. We remark that once we reduce the ξ dependence of fig. 3a to a constant, as in eq. (3.55), there is no need for further calculation. As discussed in subsect. 3.1, to this order the constant term is related to a physical quantity – the electric screening length – and so is gauge invariant. Thus the ξ dependence must cancel between diagrams.

Demonstrating that the hard thermal part of the quark self-energy is independent of ξ is even easier. The ξ-dependent term is obtained by inserting $-\xi\Delta^{\xi}_{\mu\nu}(K)$ in place of the Coulomb propagator in eq. (3.18),

$$\delta\Sigma_{\xi}(P) \approx -\xi g^2 C_{\rm f}\,{\rm Tr}\big(\gamma^{\mu}\Delta_{\rm f}(P-K)\gamma^{\nu}\Delta^{\xi}_{\mu\nu}(K)\big). \tag{3.56}$$

This term is of order $1/g$ times a hard thermal loop. We use the Ward identity for the bare quark–gluon vertex,

$$K^{\mu}\gamma^{\mu} = -i\big(\Delta_{\rm f}^{-1}(P-K) - \Delta_{\rm f}^{-1}(P)\big), \tag{3.57}$$

which is obvious since $\Delta_{\rm f}^{-1}(P) = -i\not{P}$. Applying this to both of the vertices γ^{μ} and γ^{ν} produces four terms. The term with two powers of $\Delta^{-1}(P)$ gives integrals which are g times a hard thermal loop, and so negligible. In the other terms, the propagator $\Delta_{\rm f}(P-K)$ is cancelled by one of the numerator factors $\Delta_{\rm f}^{-1}(P-K)$. After this cancellation, the remaining terms in $\delta\Sigma_{\xi}$ are at best of the same order as a hard thermal loop. Thus terms which involve $\Delta_{\rm f}^{-1}(P)$ in the numerator can be dropped. This leaves

$$\delta\Sigma_{\xi}(P) \approx i\xi g^2 C_{\rm f}\,{\rm Tr}\big(\Delta_{\rm f}^{-1}(P-K)\Delta^{2}(K)\big) \approx 0, \tag{3.58}$$

which is not a hard thermal loop. This proves that the hard thermal loop in the quark self-energy Σ is independent of ξ.

Power counting indicates that the ξ-dependent integrals contain terms which are powers of $1/g$ times a hard thermal loop. The examples of the self-energies show that the terms of order $1/g^m$ can be organized by the Ward identities so that they cancel. This generalizes directly to the ξ dependence of higher N-point functions. For example, consider the N-gluon amplitude of fig. 1a. We snip off the part of fig. 1a that contains the three-gluon vertices for the external gluons $A^{\mu_1}(P_1 - P_0)$ and $A^{\mu_2}(P_2 - P_1)$, as well as the string of three propagators which are attached to the adjacent vertices. We call this quantity $\mathscr{W}$:

$$\begin{aligned}\mathscr{W}^{\lambda_0\mu_1\mu_2\sigma_2} = {} & \Delta_{\lambda_0\sigma_0}(P_0-K)\,\Gamma^{\sigma_0\mu_1\lambda_1}(P_0-K, P_1-P_0, -P_1+K) \\ & \times\Delta_{\lambda_1\sigma_1}(P_1-K)\,\Gamma^{\sigma_1\mu_2\lambda_2}(P_1-K, P_2-P_1, -P_2+K)\,\Delta_{\lambda_2\sigma_2}(P_2-K).\end{aligned} \tag{3.59}$$

The indices λ_0 and σ_2 refer to the virtual gluon legs at the ends of the string. Each propagator is the full covariant form of eq. (3.39). Decompose $\mathscr{W}$ into the piece in the Feynman gauge, plus the ξ-dependent term: $\mathscr{W} = \mathscr{W}_F + \mathscr{W}_\xi$. In the Feynman gauge, the terms which contribute to the hard thermal loop are

$$\mathscr{W}_F^{\lambda_0\mu_1\mu_2\sigma_2} \approx \Delta(P_0 - K)\Delta(P_1 - K)\Delta(P_2 - K)\mathscr{V}^{\lambda_0\mu_1\mu_2\sigma_2}, \tag{3.60}$$

with the $\mathscr{V}$ of eq. (3.44). To obtain $\mathscr{W}_\xi$, start with the propagator in the middle of eq. (3.59), $\Delta_{\lambda_1\sigma_1}(P_1 - K)$. Now substitute the ξ-dependent piece, Δ^ξ, and use the bare Ward identity, eq. (3.50), and eqs. (3.51)–(3.53), to simplify the result. Doing so, we find

$$\begin{aligned}\mathscr{W}_\xi^{\lambda_0\mu_1\mu_2\sigma_2} \approx -\xi\big(&\Delta(P_0 - K)K^{\mu_1}(P_0 - K)^{\lambda_0}\delta^{\mu_2\sigma_2} + \Delta(P_2 - K)K^{\mu_2}(P_2 - K)^{\sigma_2}\delta^{\mu_1\lambda_0} \\ &+\Delta(P_0 - K)\Delta(P_2 - K)K^{\mu_1}K^{\mu_2}(P_0 - K)^{\lambda_0}(P_2 - K)^{\sigma_2}\big) \\ &\times\Delta^2(P_1 - K) + \ldots .\end{aligned} \tag{3.61}$$

Only the terms linear in ξ are shown. We assume that $\mathscr{W}$ is part of the N-gluon amplitude of fig. 1a at $N \geqslant 3$, which allows many terms to be dropped. For momenta tied to an external gauge index, powers of the soft P can be neglected relative to K: $(P_1 - K)^{\mu_1} \approx -K^{\mu_1}$, etc. Similarly, terms where each external μ is tied to a loop index, such as $\Delta^2(P_1 - K)\delta^{\mu_1\lambda_0}\delta^{\mu_2\sigma_2}$, do not produce a hard thermal loop, and can be ignored.

Notice that in eq. (3.61), every term is accompanied by a factor of the loop momentum for the beginning or the end of the string, tied to the appropriate loop index: either $(P_0 - K)^{\lambda_0}$, or $(P_2 - K)^{\sigma_2}$. Thus when $\mathscr{W}_\xi$ is stitched back into fig. 1a, these factors of the loop momenta continue to eat their way around the loop, in a manner such that the bare Ward identity can be applied repeatedly.

The term in the Feynman gauge, $\mathscr{W}_F$ in eq. (3.60), has three Δ's and two K's. The first two terms in $\mathscr{W}_\xi$, eq. (3.61), have the same number of Δ's and K's, and so like $\mathscr{W}_F$ produce a hard thermal loop. The last term in $\mathscr{W}_\xi$ is different: it has four Δ's and four K's, so it appears to produce integrals of order $1/g$ times a hard thermal loop. In the first two terms, though, the loop momenta is tied to its index at either the beginning or the end of the string; for the last term, this happens at both ends. Thus in the last term, the loop momenta eat their way around the diagram in both directions, and the bare Ward identity can be used to show that the possible terms of order $1/g$ cancel.

This example demonstrates that for terms proportional to ξ in the N-gluon amplitude, all terms which are $1/g$ times a hard thermal loop vanish in each individual diagram. This leaves ξ-dependent hard thermal loops. For the self-energies, once the Ward identities reduce the ξ dependence to hard thermal loops, it is simple to show that the sum vanishes when all diagrams were added together. At $N \geq 3$, there are many more diagrams, and this is not at all apparent.

To understand the cancellation of ξ-dependent hard thermal loops, we catalog the possible integrals which arise. From the diagram of fig. 1a in the Coulomb or Feynman gauge, the hard thermal loop is proportional to

$$\mathscr{J}^{\mu_1 \cdots \mu_N}(P_0, P_1, P_2, P_3, \ldots, P_{N-2}, 0) . \tag{3.62}$$

The ordering and notation is as in eq. (3.22), except that here we take $P_0 \neq 0$ and $P_{N-1} = 0$, instead of vice versa. The color factors and coupling constants do not enter into our arguments, and so are suppressed. The terms linear in ξ from fig. 1a are typified by the integral that arises from the second term in eq. (3.61),

$$\xi \mathscr{J}^{\mu_1 \cdots \mu_N}(P_1, P_1, P_2, P_3, \ldots, P_{N-2}, 0) , \tag{3.63}$$

in which the momentum P_1 is repeated, so the integral contains a double pole. For the virtual gluon line with momentum $P_1 - K$, these terms arise by replacing the Feynman propagator, Δ^{F}, with the ξ-dependent part $\xi \Delta^{\xi}$. Since Δ^{F} is proportional to Δ, and Δ^{ξ} to Δ^2, it is natural to find that for the terms linear in ξ, the same propagator appears twice. Remember, though, that it is essential to use the bare Ward identities to show that $K^{\mu} K^{\nu}$ in the numerator of $\Delta^{\xi}_{\mu\nu}(K)$ does not spoil this simple expectation.

When $\xi \neq 0$ diagrams with four-gluon interactions also produce hard thermal loops. For example, suppose one starts with fig. 1a, and removes the piece given in eq. (3.59), $\mathscr{W}^{\lambda_0 \mu_1 \mu_2 \sigma_2}$. Now sew the diagram together again with a four-gluon interaction,

$$\mathscr{W}_{4g}^{\lambda_0 \mu_1 \mu_2 \sigma_2} = \Delta_{\lambda_0 \sigma_0}(P_0 - K) \Gamma_{4g}^{\sigma_0 \mu_1 \mu_2 \lambda_2} \Delta_{\lambda_2 \sigma_2}(P_2 - K) . \tag{3.64}$$

Here Γ_{4g} denotes the four-gluon vertex with its color indices and momenta suppressed. If both propagators are Feynman propagators, $\mathscr{W}_{4g}$ does not produce a hard thermal loop. So assume that on the line with momentum $P_0 - K$, the ξ-dependent part of Δ is substituted. Power counting indicates that this diagram produces a hard thermal loop, proportional to $\xi \mathscr{J}^{\mu_1 \cdots \mu_N}(P_0, P_0, P_2, P_3, \ldots)$. The bare Ward identities show that these hard thermal loops only appear when $N \geq 4$.

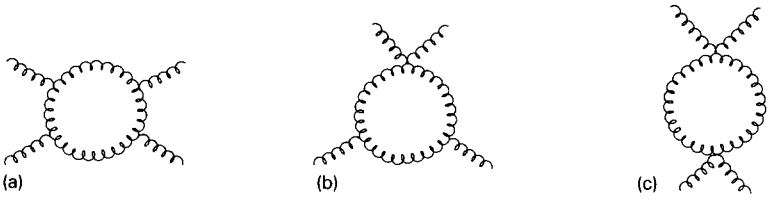

Fig. 4. One-loop diagrams which contribute to the four-gluon amplitude.

The nature of terms with higher powers of ξ is apparent. After using the bare Ward identities, terms quadratic in ξ reduce to hard thermal loops such as

$$\xi^2 \mathscr{J}^{\mu_1 \cdots \mu_N}(P_1, P_1, P_2, P_2, P_4, \ldots, P_{N-2}, 0), \tag{3.65}$$

in which there are two sets of double poles.

We assert that the sum of all ξ-dependent hard thermal loops, as in eqs. (3.63) and (3.65), vanishes in any given amplitude. This was first discovered by explicit calculation for the three- and four-gluon amplitudes. The most interesting example is the four-gluon amplitude. At one-loop order, the diagrams with a gluon loop which contribute are those of fig. 4. In the Coulomb or Feynman gauge, only the four-point form of fig. 1a, fig. 4a, contributes. Things appear much more complicated at $\xi \neq 0$: there are hard thermal loops from fig. 4a proportional to 1 and ξ, from fig. 4b proportional to ξ and ξ^2, and from fig. 4c proportional to ξ^2. Yet when these terms are added together, the terms proportional to ξ and ξ^2 cancel, leaving the result in the Feynman gauge.

This cancellation of ξ-dependent hard thermal loops, which in explicit examples seems rather mysterious, has an elementary explanation. We assume that the ξ-dependent terms cancel in the $(N-1)$-gluon amplitude, and show that they then must cancel in the N-gluon amplitude. (The same argument applies to the amplitude between a quark pair and $N-2$ gluons.) For the N-gluon amplitude, at $\xi = 0$ the hard thermal loops are like that of eq. (3.62); for $\xi \neq 0$, those of eqs. (3.63) and (3.65) appear in individual diagrams. Without loss of generality we assume that the momenta $P_0, \ldots, P_{N-2}$ are nonexceptional, so that $P_0 \neq P_1 \neq P_2 \ldots$, etc. This allows us to distinguish simply between the terms at $\xi = 0$ and $\xi \neq 0$: for terms proportional to ξ^m, the hard thermal loops which accompany them have m pairs of double poles.

The Ward identities which relate the hard thermal loops of N-gluon amplitudes to $(N-1)$-gluon amplitudes can be read off from eq. (2.40). Consider an N-gluon amplitude, where the external gluon leg $A_{\mu_1}(P_1 - P_0)$ is contracted with its

momentum, $(P_1 - P_0)^{\mu_1}$. In Feynman gauge, eq. (3.62) becomes

$$(P_1 - P_0)^{\mu_1} \mathcal{J}^{\mu_1 \cdots \mu_N}(P_0, P_1, P_2, P_3, \ldots, P_{N-2}, 0)$$
$$\approx \tfrac{1}{2}\left(\mathcal{J}^{\mu_2 \cdots \mu_N}(P_1, P_2, P_3, \ldots, P_{N-2}, 0) - \mathcal{J}^{\mu_2 \cdots \mu_N}(P_0, P_2, P_3, \ldots, P_{N-2}, 0)\right). \tag{3.66}$$

Note that both sides are free of double poles. For the term linear in ξ in eq. (3.63),

$$(P_1 - P_0)^{\mu_1} \mathcal{J}^{\mu_1 \cdots \mu_N}(P_1, P_1, P_2, \ldots, P_{N-2}, 0)$$
$$\approx \tfrac{1}{2}\left(\mathcal{J}^{\mu_2 \cdots \mu_N}(P_1, P_1, P_2, \ldots, P_{N-2}) - \mathcal{J}^{\mu_2 \cdots \mu_N}(P_1, P_2, \ldots, P_{N-2}, 0)\right)$$
$$- P_0^{\mu_1} \mathcal{J}^{\mu_1 \cdots \mu_N}(P_1, P_1, P_2, \ldots, P_{N-2}, 0). \tag{3.67}$$

There are three terms on the right-hand side. The first two are hard thermal loops for a $(N-1)$-gluon amplitude; the first has a double pole in P_1, while the second is free of double poles. The last term on the right-hand side is a hard thermal loop for a N-gluon amplitude; because the momenta are nonexceptional, it cannot be reduced any further.

With these expressions in hand, our inductive proof is trivial. By assumption, the $(N-1)$-gluon amplitude is independent of ξ, and so free of double poles. To obtain the Ward identity which relates the hard thermal loops in the N- and the $(N-1)$-gluon amplitudes, we contract with $(P_1 - P_0)^{\mu}$, which is a linear operation. Thus the only way for the sum of double poles to cancel *after* contraction is if they cancel *before* contraction. In other words, the N-gluon amplitude has no double poles, and so is independent of ξ.

In all of this we have blithely ignored color factors, which invariably complicate the detailed form of the Ward identities. For hard thermal loops, though, the Ward identities imply that the N-gluon amplitude, contracted with one of the external momenta, is a combination of $(N-1)$-gluon amplitudes. (This abbreviated Ward identity applies only to hard thermal loops, since otherwise many other things, such as ghost amplitudes, enter.) The detailed forms of the $(N-1)$-gluon amplitudes is of no consequence: however the color indices are distributed, these amplitudes remain free of double poles. All we need to know is that after contraction with P^{μ}, the sum of double poles in the N-gluon amplitude cancels, and that this contraction is a linear operation.

This concludes our proof that hard thermal loops are the same in Coulomb and covariant gauges. A more elegant proof could probably be given using functional techniques. For N-gluon amplitudes, we would start with the effective action in a soft background field, eq. (3.37). In covariant gauges, the inverse propagator that enters into eq. (3.37) depends upon ξ, and determines the ξ dependence of soft

amplitudes. Surely the approximations that we developed diagrammatically can be cast succinctly in functional form to show that $\delta S[A]$, the generating functional for hard thermal loops, is independent of ξ.

Unfortunately, we have no *physical* insight into why hard thermal loops are gauge invariant. (We assume that because they are equivalent in Coulomb and covariant gauges, this extends to arbitrary choices of gauge.) Admittedly, hard thermal loops form a very special subset of diagrams at one-loop order. But we are unaware of any other instance in nonabelian gauge theories where an entire class of diagrams is gauge invariant off mass-shell, at arbitrary momenta.

4. Resummation of hard thermal loops

In this section we develop an effective perturbation theory which resums the insertions of hard thermal loops to all orders in the loop expansion. To illustrate the use of the effective expansion, we apply it to the quark and gluon self-energies: these are the most basic quantities to compute, and have occasioned the most interest [3, 4].

The propagators and vertices in the effective expansion are defined in subsect. 4.1. They are combined in subsect. 4.2 into diagrams that give perturbative corrections to the quark and gluon self-energies, including all terms which contribute to their discontinuities at order g times the tree amplitude. The two-point $\mathscr{T}$-matrix elements are constructed by sandwiching the self-energies between physical wave functions. We establish that the two-point $\mathscr{T}$-matrix elements are gauge invariant by proving that they are equal in Coulomb and covariant gauges. In subsect. 4.3 we discuss the effective expansion beyond leading order in g, to outline the diagrams which contribute at order g and g^2 to the gluon self-energy.

4.1. EFFECTIVE PROPAGATORS AND VERTICES

We have seen that if all of the external legs in a bare amplitude are soft, then certain corrections to that amplitude – the hard thermal loops – are of the same order in g. In order to calculate consistently, this infinite subset of corrections to the bare amplitude must be included by resummation. Having isolated the contribution of hard thermal loops in sects. 2 and 3, we carry out this resummation by developing an effective perturbation expansion.

The effective expansion is similar to the usual perturbation theory, except that for soft momenta, the bare propagators and vertices are replaced by effective quantities. The effective propagators and vertices include the hard thermal loops, and are denoted by a left superscript "$*$". Topologically, many diagrams are the same as in the bare expansion. But there are also diagrams which are special to the effective expansion, being constructed out of effective vertices which have no bare counterpart.

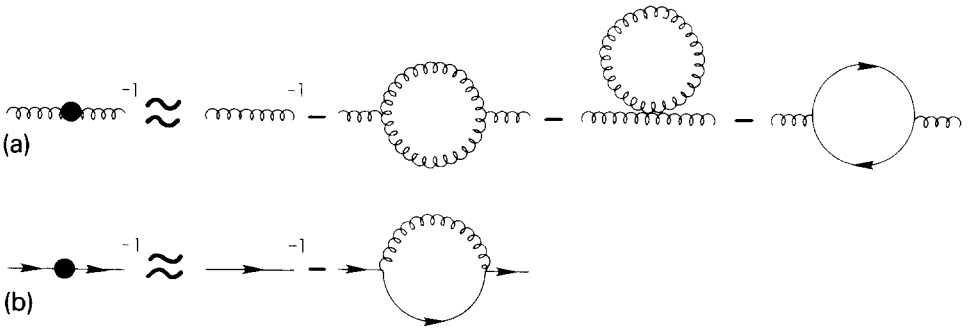

Fig. 5. The effective inverse propagators: (a) ${}^*\Delta_{\mu\nu}^{-1}$, for gluons; (b) ${}^*\Delta_{\mathrm{f}}^{-1}$, for quarks. In the one-loop diagrams of figs. 5, 6 and 7, only the hard thermal loops are included, as indicated by the symbol " $\approx$ "; just the diagrams which contribute in Coulomb gauge are shown.

The effective propagators resum all insertions of the hard thermal loop in the self energies, $\delta\Pi$ for gluons and $\delta\Sigma$ for quarks. The infinite sum of corrections to the propagator corresponds to an additive correction to the inverse propagator. The effective inverse propagator for gluons is

$$ {}^*\Delta_{\mu\nu}^{-1}(P) = \Delta_{\mu\nu}^{-1}(P) - \delta\Pi_{\mu\nu}(P) , \tag{4.1} $$

where $\delta\Pi$ is given in eq. (3.17). This is represented in fig. 5a. Like the bare inverse propagator Δ^{-1} of eq. (3.49), ${}^*\Delta^{-1}$ refers only to the transverse part of the effective inverse propagator. It is transverse in P^μ because $\delta\Pi^{\mu\nu}(P)$ satisfies the Ward identity in eq. (3.30). The complete inverse propagator is obtained by adding terms for gauge fixing, which are unaffected by resummation. The discussion of the effective gluon propagator in different gauges is deferred until the end of this subsection. The effective inverse propagator for quarks is represented in fig. 5b, and is given by

$$ {}^*\Delta_{\mathrm{f}}^{-1}(P) = \Delta_{\mathrm{f}}^{-1}(P) - \delta\Sigma(P) , \tag{4.2} $$

with the $\delta\Sigma$ of eq. (3.21). We assume that all quarks are massless; the extension to quarks with a nonzero bare mass is elementary [12].

The effective vertices are formed by adding the hard thermal loop to the bare vertex; schematically, ${}^*\Gamma = \Gamma + \delta\Gamma$. For example, for the three-gluon vertex,

$$ {}^*\Gamma^{\mu\nu\lambda}(P,Q,R) = \Gamma^{\mu\nu\lambda}(P,Q,R) + \delta\Gamma^{\mu\nu\lambda}(P,Q,R) , \tag{4.3} $$

as illustrated in fig. 6a. The hard thermal loop in the three-gluon vertex, $\delta\Gamma^{\mu\nu\lambda}$, is given in eq. (3.26). The effective three-gluon vertex has the same symmetry properties as the bare vertex. For example, it is an odd function under a change in

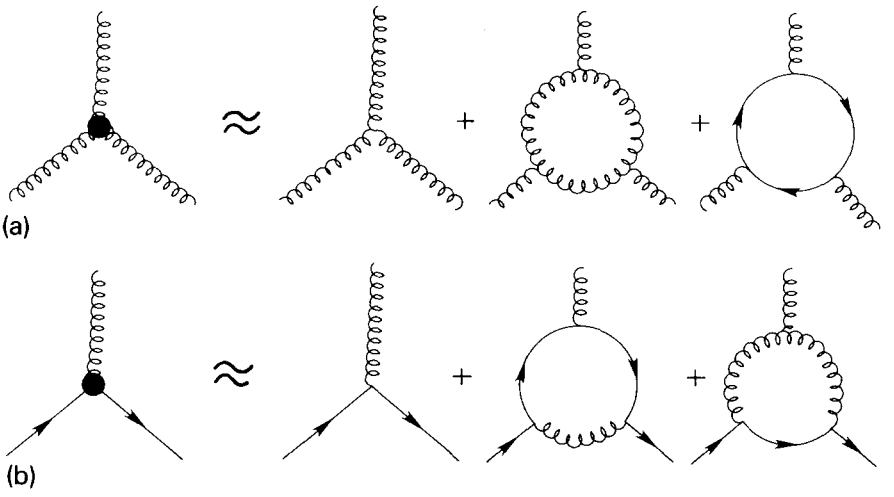

Fig. 6. The effective three-point vertices: (a) ${}^*\Gamma^{\mu\nu\lambda}$, between three gluons; (b) ${}^*\tilde{\Gamma}^{\mu}$, between a quark pair and a gluon.

sign of all the momenta,

$$ {}^*\Gamma^{\mu\nu\lambda}(-P,-Q,-R) = -{}^*\Gamma^{\mu\nu\lambda}(P,Q,R)\,, \tag{4.4} $$

and under the interchange of the momenta and Lorentz indices for two lines,

$$ {}^*\Gamma^{\nu\mu\lambda}(Q,P,R) = -{}^*\Gamma^{\mu\nu\lambda}(P,Q,R)\,. \tag{4.5} $$

The effective quark-gluon vertex ${}^*\tilde{\Gamma}^{\mu}$ is shown in fig. 6b:

$$ {}^*\tilde{\Gamma}^{\mu}(P,Q;R) = \gamma^{\mu} + \delta\tilde{\Gamma}^{\mu}(P,Q;R)\,, \tag{4.6} $$

where the hard thermal loop is that of eq. (3.27).

The effective four-gluon vertex is illustrated in fig. 7a. The component that is diagonal in the color indices of both the first pair and the last pair of gluons is

$$ {}^*\Gamma^{\mu\nu\lambda\sigma}(P,Q,R,S) = \Gamma^{\mu\nu\lambda\sigma}(P,Q,R,S) + \delta\Gamma^{\mu\nu\lambda\sigma}(P,Q,R,S)\,, \tag{4.7} $$

where $\delta\Gamma$ is given in eq. (3.28). This vertex is symmetric under interchange of momenta and Lorentz indices of the first two lines, the last two lines, and interchange of the first pair with the second pair. The vertex between a quark pair and two gluons is illustrated in fig. 7b. There is no bare vertex, so the effective vertex is given completely by the hard thermal loop. If we take the trace over the color indices of the gluons, the effective vertex ${}^*\tilde{\Gamma}^{\mu\nu} = \delta\tilde{\Gamma}^{\mu\nu}$ is given in eq. (3.29). This vertex is typical of the higher N-point vertices. There are no bare vertices for

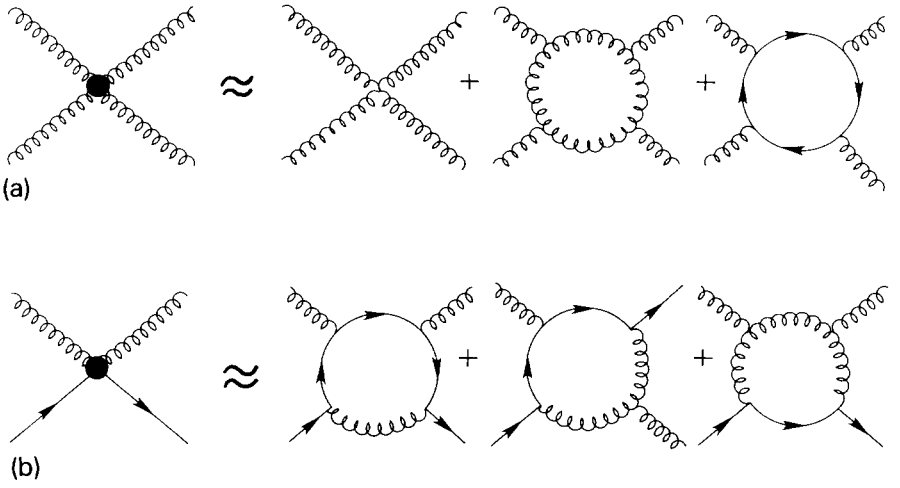

Fig. 7. The effective four-point vertices: (a) ${}^*\Gamma^{\mu\nu\lambda\sigma}$, between four gluons; (b) ${}^*\tilde{\Gamma}^{\mu\nu}$, between a quark pair and two gluons.

$N > 4$, so the effective vertices between N gluons, or between a quark pair and $N-2$ gluons, are given exclusively by the hard thermal loop.

As discussed in sect. 2, there are no hard thermal loops with ghosts on external lines, so in the effective expansion the ghost propagator and the ghost–gluon vertex remain the same as in the bare expansion.

The Ward identities satisfied by the effective vertices follow immediately from those obeyed by the hard thermal loops, eqs. (3.30)–(3.34). For the three-point amplitudes,

$$R^\lambda {}^*\Gamma^{\mu\nu\lambda}(P,Q,R) = -{}^*\Delta^{-1}_{\mu\nu}(P) + {}^*\Delta^{-1}_{\mu\nu}(Q)\,, \tag{4.8}$$

$$R^\mu {}^*\tilde{\Gamma}^{\mu}(P,Q;R) = -i\big({}^*\Delta_{\rm f}^{-1}(P) + {}^*\Delta_{\rm f}^{-1}(Q)\big)\,. \tag{4.9}$$

We require the Ward identities for the four-point vertices that are traced in the color indices of two gluons. The four-gluon vertex satisfies

$$S^\sigma {}^*\Gamma^{\mu\nu\lambda\sigma}(P,Q,R,S) = {}^*\Gamma^{\mu\nu\lambda}(P+S,Q,R) - {}^*\Gamma^{\mu\nu\lambda}(P,Q+S,R)\,. \tag{4.10}$$

For the vertex between a quark pair and two gluons, the Ward identity is

$$S^\nu {}^*\tilde{\Gamma}^{\mu\nu}(P,Q;R,S) = {}^*\tilde{\Gamma}^{\mu}(P+S,Q;R) - {}^*\tilde{\Gamma}^{\mu}(P,Q+S;R)\,. \tag{4.11}$$

What is most striking about these Ward identities is that formally they are *identical* in structure to those satisfied by the propagators and vertices at tree level.

For example, the Ward identity for the bare three-gluon vertex is given in eq. (3.50). That satisfied by the effective three-gluon vertex, eq. (4.8), is obtained merely by "starring" everything! Similarly, the Ward identity for the effective quark–gluon vertex, eq. (4.9), follows that for the bare vertex, eq. (3.57). The same can be shown for the Ward identities of the effective four-gluon vertex, eq. (4.10), and its bare counterpart. At first it seems as if the Ward identity for the vertex between a quark pair and two gluons, eq. (4.11), provides an exception, but the analogy holds even here. Since there is no bare vertex between two quarks and two gluons, $\tilde{\Gamma}^{\mu\nu} = 0$. The bare quark–gluon vertex is independent of momentum, $\tilde{\Gamma}^{\mu} = \gamma^{\mu}$. Thus eq. (4.11) applies rather trivially to the bare vertex. The simplicity of the effective Ward identities is crucial in establishing the gauge invariance of the $\mathscr{T}$-matrix elements in subsect. 4.2.

We next review [5–12] the physical interpretation of the propagating modes in the effective propagators. The effective quark propagator is obtained from eq. (4.2) directly by inversion. After analytic continuation to $k^0 = -i\omega$, the limiting behavior of the effective propagator as $k \to 0$ is

$$^*\Delta_f(K) \to \frac{\omega}{-\omega^2 + m_q^2}\left(\tfrac{1}{2}\left(\gamma^0 + i\hat{\not{k}}\right) + \tfrac{1}{2}\left(\gamma^0 - i\hat{\not{k}}\right)\right), \tag{4.12}$$

where $\hat{\not{k}} = \boldsymbol{k}\cdot\boldsymbol{\gamma}/k$. The hard thermal loop in the self-energy has produced a "mass" m_q for the quarks, where $m_q^2 = g^2 C_f T^2/8$.

The fashion in which the Dirac structure is written is deliberate. By the usual analysis [15], massless fermions which enter as $\gamma^0 + i\hat{\not{k}}$ have chirality equal to helicity; those which enter as $\gamma^0 - i\hat{\not{k}}$ have chirality equal to minus helicity. At zero temperature, the former always have positive energy, and the latter, negative energy.

Klimov and Weldon first observed that contrary to naive expectation, the pole in the effective propagator has not one but two branches at positive energy above the light cone [5, 11, 12]. The term proportional to $\gamma^0 + i\hat{\not{k}}$ is the standard mode, with chirality equal to helicity. Because of the term proportional to $\gamma^0 - i\hat{\not{k}}$, there is also a second branch with positive energy, whose chirality is equal to minus the helicity. This second branch represents a collective excitation, special to light fermions in an ultrarelativistic plasma [5, 12]. At $k = 0$ these two branches are degenerate, but they diverge away from zero momentum. In both cases the effective mass shells do not have a relativistically invariant form, which is why we refer to the quark "mass" in quotes. For $k \gg m_q$, each branch approaches the light cone, and so the fields become essentially massless. As written in eq. (4.12), at zero momentum the residue of each mode is one-half the usual value. When $k \gg m_q$, the residue of the standard branch approaches one, while that for the collective mode vanishes exponentially. The detailed forms can be found elsewhere [5, 11, 12].

Unlike the effective quark propagator, the form of the effective gluon propagator depends upon the gauge. By the Ward identity of eq. (3.30), the hard thermal loop in the gluon self-energy is transverse in K. At nonzero temperature the gluon self-energy has two independent components, longitudinal and transverse. The hard thermal loop in the gluon self-energy can be decomposed accordingly:

$$\delta\Pi^{00}(K) = \delta\Pi_{\ell}(K), \qquad \delta\Pi^{0i}(K) = -\frac{k^0 k^i}{k^2}\delta\Pi_{\ell}(K),$$

$$\delta\Pi^{ij}(K) = (\delta^{ij} - \hat{k}^i\hat{k}^j)\delta\Pi_{t}(K) + \hat{k}^i\hat{k}^j\frac{(k^0)^2}{k^2}\delta\Pi_{\ell}(K), \tag{4.13}$$

where $\delta\Pi_{\ell}$ is the longitudinal and $\delta\Pi_{t}$ the transverse components.

The effective gluon propagator is obtained by adding gauge-fixing terms to eq. (4.1), and then inverting it. The physical excitations of the gluon are most transparent in strict Coulomb gauge, where $\xi_C = 0$:

$$^*\Delta_C^{00}(K) = {}^*\Delta_{\ell}(K), \qquad {}^*\Delta_C^{0i}(K) = 0,$$

$$^*\Delta_C^{ij}(K) = (\delta^{ij} - \hat{k}^i\hat{k}^j)\,{}^*\Delta_{t}(K). \tag{4.14}$$

We have introduced the transverse and longitudinal propagators,

$${}^*\Delta_{t}(K) = \frac{1}{K^2 - \delta\Pi_{t}(K)}, \qquad {}^*\Delta_{\ell}(K) = \frac{1}{k^2 - \delta\Pi_{\ell}(K)}, \tag{4.15}$$

with $K^2 = (k^0)^2 + k^2$. When $\xi_C \neq 0$, the Coulomb propagator is given by adding $\xi_C K^\mu K^\nu/(k^2)^2$ to the ${}^*\Delta_C^{\mu\nu}(K)$ of eq. (4.14).

The transverse propagator ${}^*\Delta_{t}$ represents the two physical degrees of freedom of a field with spin one. When $k^0 = -i\omega$ and the momentum k goes to zero,

$${}^*\Delta_{t}(K) \to \frac{1}{-\omega^2 + m_g^2}, \tag{4.16}$$

where m_g is the gluon "mass", $m_g^2 = (N_c + N_f/2)(gT)^2/9$. Physically, $1/m_g$ is the frequency at which time-dependent magnetic fields are screened over large distances. The pole in the transverse propagator approaches the light cone at large momentum k; its residue times ω is of order one at all momenta.

The longitudinal degree of freedom, with propagator ${}^*\Delta_{\ell}$, plays a special role at nonzero temperature. At zero temperature it can often be ignored: because it is a static mode, it produces the familiar Coulomb interaction, but does not contribute to discontinuities. At nonzero temperature, however, the hard thermal loop in the

longitudinal self-energy turns it into a propagating mode. As $k \to 0$, the effective longitudinal propagator behaves as

$$^*\Delta_\ell(K) \to \frac{-\omega^2}{k^2} \frac{1}{-\omega^2 + m_g^2} . \tag{4.17}$$

The longitudinal and transverse modes have the same "mass" m_g: over large distances, the screening frequency for time-dependent electric and magnetic fields are equal. The propagation of the longitudinal mode is a collective effect, completely analogous to the same mode in a nonrelativistic plasma. The mass shells for the longitudinal and transverse modes differ at nonzero momentum. Notably, the longitudinal mode only contributes significantly to discontinuities at soft momentum, for when $p \gg m_g$ its residue is exponentially small [12].

In covariant gauge the propagator is obtained by adding the gauge-fixing term $-(1-\xi)K^\mu K^\nu$ to eq. (4.1) and inverting. For our purposes it is most convenient to express the propagator in covariant gauge in terms of its difference from Coulomb gauge:

$$^*\Delta^{\mu\nu}(K) = {}^*\Delta_C^{\mu\nu}(K) + K^\mu K^\nu {}^*\Delta_1(K) + (n^\mu K^\nu + K^\mu n^\nu) {}^*\Delta_2(K) , \tag{4.18}$$

where n^μ is a unit vector such that $n^\mu K^\mu = k^0$, and the last two terms are

$$^*\Delta_1(K) = \frac{\xi}{(K^2)^2} - \frac{\xi_C}{(k^2)^2} + \frac{(k^0)^2}{(K^2)^2} {}^*\Delta_\ell(K) ,$$

$$^*\Delta_2(K) = -\frac{k^0}{K^2} {}^*\Delta_\ell(K) . \tag{4.19}$$

The transverse mode, $^*\Delta_t$, enters in the same manner in any covariant or Coulomb gauge. In contrast, in covariant gauge the longitudinal mode $^*\Delta_\ell$ appears not only in $^*\Delta_{00}$, as in Coulomb gauge, eq. (4.14), but it also appears in each term of the difference in (4.18).

The role of the longitudinal mode can be clarified by the example of an abelian gauge field coupled to a conserved, external current J^μ, as considered by Weldon [11] and Pisarski [12]. The effective action in the presence of this current is

$$S_J = \tfrac{1}{2} J^\mu {}^*\Delta^{\mu\nu} J^\nu = \tfrac{1}{2} J^\mu {}^*\Delta_C^{\mu\nu} J^\nu . \tag{4.20}$$

The covariant propagator $^*\Delta$ can be replaced by the Coulomb propagator $^*\Delta_C$ because, by eq. (4.18), every term in the difference is proportional to either K^μ or K^ν, and these terms vanish when sandwiched between conserved currents, $K^\mu J^\mu = 0$. This shows that in the covariant propagator, the longitudinal mode, $^*\Delta_\ell$, appears

in both physical and unphysical terms. Only that term identical to ${}^*\Delta_C^{00}$ is physical, as it contributes to a physical quantity, S_J. All of the other ways in which ${}^*\Delta_\ell$ enters in the covariant propagator, through ${}^*\Delta_1$ and ${}^*\Delta_2$, are unphysical.

This example illustrates another important point. The transverse mode in ${}^*\Delta_t$ is a typical physical excitation, with positive residue on mass-shell. In contrast, the longitudinal mode has negative residue on its mass-shell [5, 12]. This can be seen by comparing eqs. (4.16) and (4.17): about zero momentum the residue of the longitudinal mode is $-\omega^2/k^2 \simeq -m_g^2/k^2$ times that for the transverse mode. In Coulomb gauge, however, the longitudinal mode couples only to the time-like component of the current; through $J^0 {}^*\Delta_C^{00} J^0/2$ in S_J. With our euclidean conventions J^0 is imaginary on mass-shell, and $(J^0)^2$ negative, so in all the contribution of the longitudinal mode to physical quantities is positive – just like that of the transverse modes.

The effective propagators and vertices define a perturbative expansion which resums all hard thermal loops. The effective expansion is defined diagrammatically, as in ordinary perturbation theory, except that when the momenta are soft, the bare propagators and vertices are replaced by effective propagators and vertices. In loop diagrams, the integrals over virtual momenta must be separated into those over soft and over hard momenta. (The need for this is discussed more fully in subsect. 4.3.) Each soft line requires an effective propagator; bare propagators are used for hard lines. If all the legs of a vertex are soft, an effective vertex is needed; a bare vertex is used if two or more legs are hard.

It should be evident that within the effective expansion, loop corrections are down by at least one power of g. In the bare expansion, the only diagrams which are as large as a tree amplitude are the hard thermal loops, which arise for amplitudes in which every leg is soft. By resumming these into the effective propagators and vertices, all that remains are corrections of order g times the tree amplitude. Thus the effective expansion defines a power series in g, where only a finite number of diagrams contribute to any fixed order in g. Loop corrections in the effective expansion are discussed further in subsect. 4.3.

While the mathematical expressions for diagrams with effective propagators and vertices are considerably more complicated than their bare counterparts, they can be used for practical calculations. In any loop the integration over loop momenta is divided into a sum of the integral over soft k, $\mathrm{Tr}_{(\mathrm{soft})}$, and the integral over hard k, $\mathrm{Tr}_{(\mathrm{hard})}$. Like in bare perturbation theory, it is convenient to do the discrete sum over k^0 noncovariantly. This requires that the effective propagators and vertices be Fourier transformed from functions of k^0 into functions of τ, as in eq. (2.3) [5, 12, 14]. Fourier transformation generates a spectral representation for an effective quantity in the form of the integral of a spectral density, $\rho(\omega, k)$, with respect to a spectral parameter ω. The spectral representations required for the explicit evaluation of diagrams are left to another work [14]. At present we only need to know that the form of the spectral densities is such that ω is always of the same

order as k. Hence we can use the spatial momentum k to characterize whether a line carries soft or hard momentum. Doing the sum over k^0 and the integrals over τ is no more difficult than for the bare expansion, since all of the complications of the effective expansion reside in the spectral densities. It remains only to integrate over k and over the spectral parameters ω, with the integrand a product of spectral densities, energy denominators, and statistical distribution functions. In this form, even after analytic continuation it is safe to estimate a diagram by power counting.

The effective propagators and vertices define a nonlocal effective field theory which can be understood intuitively as the result of a renormalization group transformation. Divide the original theory into fields with hard and fields with soft momenta. As discussed in subsect. 3.1 preceding eq. (3.37), integrating out all fields with hard momenta produces an effective theory for fields with soft momenta. Keeping only the contribution of hard thermal loops, and discarding all terms which are down by powers of g, produces the above effective theory. In this light, the appearance of new vertices merely represents the expansion of the effective action at one-loop order in powers of the soft A field.

We conclude this subsection by noting that the effective expansion can alternately be derived as an approximate solution to the Schwinger–Dyson equations. The effective vertices and propagators represent approximate solutions to the exact quantities. In the effective expansion, an effective vertex is required whenever all of the momenta going into a vertex are soft. In the Schwinger–Dyson equations, though, both bare and exact vertices appear, even when the loop momentum is soft. The loop integrals in the Schwinger–Dyson equations run over all momenta, hard and soft. It can be shown that the integral over hard momentum generates a hard thermal loop, which combines with the bare vertex to form the usual effective vertex. Our original view – constructing the effective expansion by integrating out all hard thermal fluctuations – is both more direct and more natural.

4.2. GAUGE INVARIANCE OF $\mathscr{S}$-MATRIX ELEMENTS

In this section we use the effective expansion to write down expressions for the one-loop corrections to the quark and gluon self-energies at soft momentum. These expressions include all terms that contribute at order g to the discontinuities in the self-energies. We construct two-point $\mathscr{S}$-matrix elements from these self-energies, and use the Ward identities to establish their equality in covariant and Coulomb gauges. This proves that the damping rates are gauge invariant to lowest order in g.

As we discuss in subsect. 4.3, there are three classes of diagrams which contribute at order g to the self-energy: one-loop diagrams with soft loop momentum, and one- and two-loop diagrams, in which all loop momenta are hard. Our

principal interest is in the damping rates, which are due to the discontinuities of the self-energy on the mass-shell. At order g, the discontinuity arises only from the soft one-loop diagrams, and so we concentrate on them in this subsection.

Power counting shows that soft one-loop diagrams contribute to the self-energies at order g. For soft momenta, our effective propagators and vertices are of the same order as their bare counterparts, so the power counting of soft loop diagrams in the effective expansion is the same as for bare diagrams in the bare expansion. If both the external and the loop momenta are soft, all momenta in the diagram are of order gT. Thus to estimate a diagram, we need only keep track of the powers of g and the behavior of the statistical distribution functions. In one-loop diagrams, only single powers of the statistical distribution functions, $n(E)$ and $\tilde{n}(E)$, appear: for soft E, $n(E) \simeq T/E \sim 1/g$ and $\tilde{n}(E) \simeq 1/2$. Thus soft one-loop diagrams with at least one gluon line are of order $g^2 n(E) \sim g$. Those involving just quark lines, and so Fermi–Dirac distribution functions, are of order $g^2 \tilde{n}(E) \sim g^2$.

We first discuss the effective self-energy for the gluon, ${}^*\Pi^{\mu\nu}$, which includes leading corrections to the effective propagator, ${}^*\Delta^{\mu\nu}$. There are three diagrams with soft loop momenta which contribute at order g:

$$ {}^*\Pi^{\mu\nu}(P) = {}^*\Pi^{\mu\nu}_{3g}(P) + {}^*\Pi^{\mu\nu}_{4g}(P) + {}^*\Pi^{\mu\nu}_{gh}(P) . \tag{4.21} $$

${}^*\Pi_{3g}$ is given by the graph in fig. 8a with two effective three-gluon interactions,

$$ {}^*\Pi^{\mu\nu}_{3g}(P) = -\frac{g^2 N_c}{2} \mathrm{Tr}_{(\mathrm{soft})} {}^*\Gamma^{\sigma\mu\lambda}(-P+K, P, -K) {}^*\Delta^{\lambda\lambda'}(K) $$

$$ \times {}^*\Gamma^{\lambda'\nu\sigma'}(-K, P, -P+K) {}^*\Delta^{\sigma'\sigma}(P-K) . \tag{4.22} $$

${}^*\Pi_{4g}$ is given by the graph with an effective four-gluon interaction, fig. 8b,

$$ {}^*\Pi^{\mu\nu}_{4g}(P) = -\frac{g^2 N_c}{2} \mathrm{Tr}_{(\mathrm{soft})} {}^*\Gamma^{\mu\nu\lambda\sigma}(P, -P, K, -K,) {}^*\Delta^{\lambda\sigma}(K) . \tag{4.23} $$

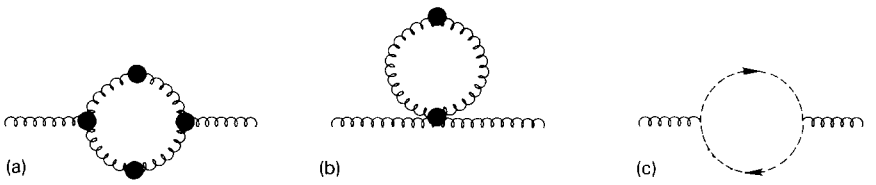

Fig. 8. One-loop diagrams which contribute to the effective gluon self-energy, ${}^*\Pi^{\mu\nu}$.

Lastly there is the contribution of the ghost loop in fig. 8c,

$$^*\Pi^{\mu\nu}_{\rm gh}(P) = g^2 N_{\rm c}\,{\rm Tr}_{\rm (soft)} K^\mu (P-K)^\nu \Delta(K)\Delta(P-K)\,. \tag{4.24}$$

In figs. 8a and 8b, all propagators and vertices are dotted to denote that they are effective quantities. Since ghost amplitudes do not have hard thermal loops, nothing in the ghost loop of fig. 8c is dotted.

The effective self-energy $^*\Pi^{\mu\nu}$ of eq. (4.21) is that of covariant gauge: in eqs. (4.22) and (4.23), every gluon propagator is covariant. In the Coulomb gauge, the effective self-energy equals

$$^*\Pi^{\mu\nu}_{\rm C}(P) = {}^*\Pi^{\mu\nu}_{\rm C,3g}(P) + {}^*\Pi^{\mu\nu}_{\rm C,4g}(P) + {}^*\Pi^{\mu\nu}_{\rm C,gh}(P)\,. \tag{4.25}$$

$^*\Pi^{\mu\nu}_{\rm C,3g}$ and $^*\Pi^{\mu\nu}_{\rm C,4g}$ are given just by replacing covariant with Coulomb gauge propagators everywhere in eqs. (4.22) and (4.23). The ghosts are static in Coulomb gauge, and contribute only when the indices μ and ν are spatial:

$$^*\Pi^{ij}_{\rm C,gh}(P) = g^2 N_{\rm c}\,{\rm Tr}_{\rm (soft)} \frac{k^i (p-k)^j}{k^2 (p-k)^2}\,. \tag{4.26}$$

For generic momentum P, the effective self-energies are gauge dependent: $^*\Pi^{\mu\nu}$ varies with ξ, $^*\Pi^{\mu\nu}_{\rm C}$ varies with $\xi_{\rm C}$, and $^*\Pi^{\mu\nu} \neq {}^*\Pi^{\mu\nu}_{\rm C}$.

The position of the pole in a propagator is a physical quantity, and therefore gauge invariant. At lowest order the mass-shell conditions are defined by the poles in the effective propagators. For gluons, a physical polarization vector obeys

$$^*\Delta^{-1}_{\mu\nu}(P) e^\nu(P)\big|_{\rm mass\text{-}shell} = 0\,, \tag{4.27}$$

where $^*\Delta^{-1}_{\mu\nu}$, eq. (4.1), is the transverse part of the effective inverse propagator. Since $^*\Delta^{-1}_{\mu\nu}$ is gauge invariant, so is the mass-shell condition which it defines. Whenever $e^\mu(P)$ appears in an equation, implicitly P^μ is on the appropriate mass-shell. At nonzero temperature $e^\mu(P)$ has three independent components – two for the transverse modes, and one for the longitudinal mode. While $^*\Delta^{-1}_{\mu\nu}$ is independent of gauge, the wave functions are not. The covariant gauge wave function satisfies $P^\mu e^\mu(P) = 0$, while the Coulomb gauge wave function obeys $p^i e^i_{\rm C}(P) = 0$. The two are related as

$$e^\mu_{\rm C}(P) = e^\mu(P) - P^\mu \frac{\boldsymbol{p}\cdot\boldsymbol{e}(P)}{p^2}\,. \tag{4.28}$$

The corrections of order g to the mass-shell are determined by the effective self-energy $^*\Pi^{\mu\nu}$, which also contains gauge variant information. To isolate the gauge invariant terms in $^*\Pi^{\mu\nu}$ which shift the mass-shell, we construct the two gluon $\mathscr{T}$-matrix element. This is formed by putting $^*\Pi^{\mu\nu}$ on the mass-shell of eq. (4.27) and sandwiching it between physical wave functions. In covariant gauge this $\mathscr{T}$-matrix element is

$$\mathscr{T} = e^{\mu} {}^*\Pi^{\mu\nu} e^{\nu} . \tag{4.29}$$

$\mathscr{T}$ is of course a function of the momentum P, but for notational ease, in this equation and henceforth we assume that each $\mathscr{T}$, $^*\Pi^{\mu\nu}$, e^{μ}, etc., are functions of P alone, and so drop their explicit dependence on P. We also omit the index i labelling the distinct polarization vectors e_i^{μ} and the corresponding indices on $\mathscr{T}_{ij}$. The terms in $^*\Pi^{\mu\nu}$ which are proportional to $^*\Delta_{\mu\nu}^{-1}$ are gauge variant: they do not contribute to $\mathscr{T}$, but produce wave function renormalization. The terms in $^*\Pi^{\mu\nu}$ which contribute to $\mathscr{T}$ are gauge invariant, and shift the position of the pole away from the mass-shell condition in eq. (4.27), by an amount of order g^3T^2. The shift in the real part of the pole represents a perturbative correction to the inverse screening length m_g. The shift in the imaginary part of the pole is proportional to the damping rate.

In the Coulomb gauge the $\mathscr{T}$-matrix element is

$$\mathscr{T}_C = e_C^{\mu} {}^*\Pi_C^{\mu\nu} e_C^{\nu} . \tag{4.30}$$

To establish gauge invariance we need to prove that $\mathscr{T} = \mathscr{T}_C$. Our proof of gauge invariance exploits the Ward identities satisfied by the effective vertices. As we noted in subsect. 4.1, these Ward identities have the same structure as the Ward identities for the bare vertices; thus our proof involves exactly the same manipulations as are required at zero temperature.

As a preliminary step in the proof, we establish the identities

$$P^{\mu} {}^*\Pi^{\mu\nu} P^{\nu} = 0, \qquad P^{\mu} {}^*\Pi^{\mu\nu} e^{\nu} = 0 . \tag{4.31), (4.32}$$

The first relation is a Ward identity that holds for arbitrary P^{μ}, and shows that $^*\Pi^{\mu\nu}$ is transverse in P^{μ}. The second identity applies only on mass-shell. The proofs of eqs. (4.31) and (4.32) are essentially the same. In each case, the Ward identities are used to reduce the contraction of P^{μ} with a three- or four-gluon vertex. After using these Ward identities, terms proportional to $^*\Delta_{\mu\nu}^{-1}(P)$ appear. But these terms vanish whether $^*\Delta_{\mu\nu}^{-1}(P)$ is contracted with P^{ν}, because $^*\Delta^{-1}(P)$ is transverse, or with e^{ν}, by the definition of the wave function. It therefore suffices to prove eq. (4.32).

For the contribution of the diagram in fig. 8a, eq. (4.22), the Ward identity of eq. (4.8) can be used to replace $P^{\mu} {}^*\Gamma^{\sigma\mu\lambda}$ by $^*\Delta_{\sigma\lambda}^{-1}(P-K) - {}^*\Delta_{\sigma\lambda}^{-1}(K)$. After shifting

the variable of integration $K \to P - K$, we see that both terms are equal, and give

$$P^\mu {}^*\Pi_{3g}^{\mu\nu} e^\nu = g^2 N_c \, \mathrm{Tr}_{(\mathrm{soft})} {}^*\Delta^{\sigma'\sigma}(P-K) {}^*\Delta^{-1}_{\sigma\lambda}(P-K) \times {}^*\Delta^{\lambda\lambda'}(K) {}^*\Gamma^{\lambda'\nu\sigma'}(-K, P, -P+K) e^\nu . \tag{4.33}$$

For the diagram of fig. 8b, eq. (4.23), the Ward identity of eq. (4.10) is used to express $P^\mu {}^*\Gamma^{\mu\nu\lambda\sigma}$ as the sum of two terms, which are again equal after a shift in K:

$$P^\mu {}^*\Pi_{4g}^{\mu\nu} e^\nu = g^2 N_c \, \mathrm{Tr}_{(\mathrm{soft})} {}^*\Delta^{\lambda\sigma}(K) {}^*\Gamma^{\sigma\nu\lambda}(-K, P, -P+K) e^\nu . \tag{4.34}$$

To reduce eq. (4.33), we use the identity

$${}^*\Delta^{-1}_{\mu\lambda}(K) {}^*\Delta^{\lambda\nu}(K) = \delta^{\mu\nu} - K^\mu K^\nu \Delta(K) . \tag{4.35}$$

This has the same form as the similar relation for the bare quantities, eq. (3.51). It is more striking here, since while the left-hand side involves the (complicated) effective propagators in covariant gauge, the right-hand side does not. Using this identity, we find that

$$P^\mu \left({}^*\Pi_{3g}^{\mu\nu} + {}^*\Pi_{4g}^{\mu\nu} \right) e^\nu = g^2 N_c \, \mathrm{Tr}_{(\mathrm{soft})} \Delta(P-K) (P-K)^\lambda {}^*\Delta_{\lambda\sigma}(K) \times {}^*\Gamma^{\sigma\nu\lambda'}(-K, P, -P+K) (P-K)^{\lambda'} e^\nu . \tag{4.36}$$

We can use the Ward identity again to replace $(P-K)^{\lambda'} {}^*\Gamma^{\sigma\nu\lambda'}$ by ${}^*\Delta^{-1}_{\sigma\nu}(P) - {}^*\Delta^{-1}_{\sigma\nu}(K)$. The first term vanishes upon contraction with e^ν (or P^ν), while eq. (4.35) can be used to simplify the latter. Eq. (4.36) becomes

$$P^\mu \left({}^*\Pi_{3g}^{\mu\nu} + {}^*\Pi_{4g}^{\mu\nu} \right) e^\nu = g^2 N_c \, \mathrm{Tr}_{(\mathrm{soft})} \Delta(P-K) (P-K)^\mu \left(\delta^{\mu\nu} - K^\mu K^\nu \Delta(K) \right) e^\nu . \tag{4.37}$$

Thus we obtain an expression involving only bare quantities, free of effective propagators and vertices. It is then easy to show that eq. (4.37) cancels against the contribution of the ghost loop, $P^\mu {}^*\Pi_{gh}^{\mu\nu} e^\nu$. This completes the proof of eq. (4.32).

The proof of gauge invariance for the two-point $\mathscr{T}$-matrix element proceeds in two steps. First we need to show that in the Coulomb $\mathscr{T}$-matrix element of eq. (4.30), Coulomb can be replaced by covariant wave functions:

$$\mathscr{T}_C = e^\mu {}^*\Pi_C^{\mu\nu} e^\nu . \tag{4.38}$$

This is demonstrated by proving the identities of eqs. (4.31) and (4.32) for the effective self-energy in the Coulomb gauge, ${}^*\Pi_C^{\mu\nu}$; then eq. (4.38) follows easily from eq. (4.28). The second step in the proof is to show that for the covariant $\mathscr{T}$-matrix element, eq. (4.29), the effective self-energy ${}^*\Pi^{\mu\nu}$ can be replaced by its

counterpart in the Coulomb gauge:

$$\mathscr{T} = e^{\mu} {}^{*}\Pi_{\mathrm{C}}^{\mu\nu} e^{\nu} . \tag{4.39}$$

Then evidently, $\mathscr{T} = \mathscr{T}_{\mathrm{C}}$.

The proof of eq. (4.39) involves the same type of manipulations as above, so we can afford to be sketchy. The difference between the covariant and Coulomb propagators is given in eq. (4.18): each term involves at least one power of either K^{μ} or K^{ν}. For instance, in eq. (4.22), the difference ${}^{*}\Delta^{\sigma\sigma'}(P-K) - {}^{*}\Delta_{\mathrm{C}}^{\sigma\sigma'}(P-K)$ includes a term proportional to $(P-K)^{\sigma}$. When contracted with ${}^{*}\Gamma^{\sigma\mu\lambda}$, it reduces to ${}^{*}\Delta_{\mu\lambda}^{-1}(P) - {}^{*}\Delta_{\mu\lambda}^{-1}(K)$ by the Ward identity of eq. (4.8). The first term, ${}^{*}\Delta_{\mu\lambda}^{-1}(P)$, vanishes when contracted with e^{μ}. The second term is simplified by using eq. (4.35). Continuing in this way, it can be shown that

$$\begin{aligned}
\mathscr{T}_{3\mathrm{g}} - \mathscr{T}_{\mathrm{C},3\mathrm{g}} = g^2 N_{\mathrm{c}} e^{\mu} \operatorname{Tr}_{(\mathrm{soft})} \Big[& {}^{*}\Delta_1(K) {}^{*}\Delta_{\mu\nu}^{-1}(P-K) \\
& - {}^{*}\Delta_2(K) \Big({}^{*}\Gamma^{\nu\mu\lambda}(-P+K, P, -K) n^{\lambda} + n^{\sigma} {}^{*}\Gamma^{\sigma\nu\mu}(K, -P, P-K) \\
& \times \Delta(P-K)(P-K)^{\mu} n^{\lambda} {}^{*}\Delta_{\lambda\nu}^{-1}(K) + \Delta(P-K) {}^{*}\Delta_{\mu\sigma}^{-1}(K) n^{\sigma} (P-K)^{\nu} \Big) \\
& + {}^{*}\Delta_2(K) {}^{*}\Delta_2(P-K) {}^{*}\Delta_{\mu\lambda}^{-1}(P-K) n^{\lambda} n^{\sigma} {}^{*}\Delta_{\sigma\nu}^{-1}(K) \Big] e^{\nu} .
\end{aligned} \tag{4.40}$$

We define $\mathscr{T}_{3\mathrm{g}} = e^{\mu} {}^{*}\Pi_{3\mathrm{g}}^{\mu\nu} e^{\nu}$, etc. The first terms in eq. (4.40) are cancelled by the contribution from the four-gluon vertex:

$$\begin{aligned}
\mathscr{T}_{4\mathrm{g}} - \mathscr{T}_{\mathrm{C},4\mathrm{g}} = g^2 N_{\mathrm{c}} e^{\mu} \operatorname{Tr}_{(\mathrm{soft})} \Big[& - {}^{*}\Delta_1(K) {}^{*}\Delta_{\mu\nu}^{-1}(P-K) \\
& + {}^{*}\Delta_2(K) \Big({}^{*}\Gamma^{\nu\mu\lambda}(-P+K, P, -K) n^{\lambda} + n^{\sigma} {}^{*}\Gamma^{\sigma\nu\mu}(K, -P, P-K) \Big) \Big] e^{\nu} .
\end{aligned} \tag{4.41}$$

Lastly, there is the difference between the ghost loops in covariant and Coulomb gauge:

$$\begin{aligned}
\mathscr{T}_{\mathrm{gh}} - \mathscr{T}_{\mathrm{C},\mathrm{gh}} = g^2 N_{\mathrm{c}} e^{\mu} \operatorname{Tr}_{(\mathrm{soft})} \Bigg[& K^{\mu} (P-K)^{\nu} \Delta(K) \Delta(P-K) \\
& - \frac{1}{k^2 (\boldsymbol{p}-\boldsymbol{k})^2} (K^{\mu} - k^0 n^{\mu}) \big((P-K)^{\nu} - (p-k)^0 n^{\nu} \big) \Bigg] e^{\nu} .
\end{aligned} \tag{4.42}$$

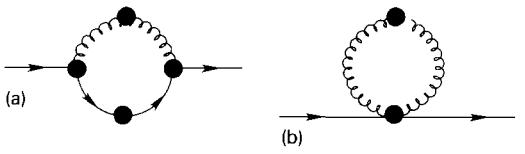

Fig. 9. One-loop diagrams which contribute to the effective quark self-energy, $^*\Sigma$.

To further reduce eq. (4.40), we employ the relation

$$^*\Delta^{-1}_{\mu\nu}(K)n^\nu = \frac{1}{k^2\,{}^*\Delta_\ell(K)}(K^2 n^\mu - k^0 K^\mu)\,. \tag{4.43}$$

Using this identity, it can be shown that the sum of eqs. (4.40)–(4.42) vanishes. This completes the proof of eq. (4.39), and so of the gauge invariance of the two-gluon $\mathscr{T}$-matrix.

The treatment of the quark self-energy is similar. The effective self-energy for quarks, $^*\Sigma(P)$, includes leading corrections to the effective quark propagator, $^*\Delta_{\rm f}(P)$. There are two diagrams with soft loop momenta which contribute at order g:

$$^*\Sigma(P) = {}^*\Sigma_3(P) + {}^*\Sigma_4(P)\,. \tag{4.44}$$

$^*\Sigma_3$, in fig. 9a, is the usual self-energy graph at one-loop order, except that all of the vertices and propagators are effective:

$$\begin{aligned} ^*\Sigma_3(P) = {} & -g^2 C_{\rm f}\,{\rm Tr}_{\rm (soft)}\,{}^*\Gamma^\mu(P, -P+K; -K)\,{}^*\Delta_{\rm f}(P-K) \\ & \times {}^*\Gamma^\nu(-P, P-K; K)\,{}^*\Delta^{\mu\nu}(K)\,. \end{aligned} \tag{4.45}$$

Σ_4 comes from a second graph, fig. 9b, which is special to the effective expansion. It arises from the effective vertex between two gluons and a quark pair:

$$^*\Sigma_4(P) = -i\frac{g^2 C_{\rm f}}{2}\,{\rm Tr}_{\rm (soft)}\,{}^*\tilde{\Gamma}^{\mu\nu}(P, -P; K, -K)\,{}^*\Delta^{\mu\nu}(K)\,. \tag{4.46}$$

Like the gluon self-energy, there are also one- and two-loop diagrams with hard loop momentum which contribute to the real – but not the imaginary – part of the self-energies at order g.

The expressions in eqs. (4.45) and (4.46) are valid in covariant gauge. The effective quark self-energy in Coulomb gauge, $^*\Sigma_{\rm C} = {}^*\Sigma_{\rm C,3} + {}^*\Sigma_{\rm C,4}$ is obtained by replacing the covariant with Coulomb propagators in eqs. (4.45) and (4.46). For generic momenta P, the effective self-energies are gauge dependent.

The $\mathscr{T}$-matrix for a quark pair is obtained by putting the effective self-energy $^*\Sigma$ on mass-shell, and sandwiching it between quark wave functions. The mass-shell

and the quark wave functions are defined by

$$^*\Delta_f^{-1}(P)\psi(P)\big|_{\text{mass-shell}} = 0. \tag{4.47}$$

Whenever $\psi(P)$ appears in an equation, implicitly P^μ is on the mass-shell. The quark wave functions do not depend upon gauge. As discussed following eq. (4.12), there are two branches to the quark mass-shell. We do not distinguish which branch the wave function $\psi(P)$ belongs to. The $\mathscr{T}$-matrix for a quark pair is

$$\tilde{\mathscr{T}} = \bar{\psi}\,{}^*\Sigma\psi\,, \tag{4.48}$$

where $\tilde{\mathscr{T}}$, $^*\Sigma$ and ψ are implicitly functions of P.

In Coulomb gauge the corresponding $\mathscr{T}$-matrix element, $\tilde{\mathscr{T}}_C$, is given by replacing $^*\Sigma$ with $^*\Sigma_C$ in eq. (4.48). We again exploit the Ward identities to prove that $\tilde{\mathscr{T}} = \tilde{\mathscr{T}}_C$. For example, when a term in the gluon propagator proportional to K^μ or K^ν is contracted with a vertex between a quark pair and a gluon, eq. (4.9) is used. Some of the resulting terms contain $\Delta_f^{-1}(P)$, and vanish by eq. (4.47). The remaining terms reduce to

$$\tilde{\mathscr{T}}_3 - \tilde{\mathscr{T}}_{C,3} = -ig^2 C_F \bar{\psi}\,\mathrm{Tr}\big(^*\Delta_1(K)K^\nu + 2^*\Delta_2(K)n^\nu\big)^*\Gamma^\nu(-P, P-K; K)\psi\,, \tag{4.49}$$

for $\tilde{\mathscr{T}}_3 = \bar{\psi}\,{}^*\Sigma_3\psi$, etc. The terms from fig. 9b, $\tilde{\mathscr{T}}_4 - \tilde{\mathscr{T}}_{C,4}$, are simplified by using the Ward identity of eq. (4.11). This term, which has no analogy at zero temperature, exactly cancels eq. (4.49).

This completes the proof that $\tilde{\mathscr{T}}$ is gauge invariant; it also shows that to leading order in g, the quark damping rate is gauge invariant. The extension to quarks with nonzero bare mass is direct [5, 12]. For light quarks with a soft mass of order gT, the hard thermal loops are unaffected, so the bare mass is just included in $^*\Delta_f^{-1}$, eq. (4.2). Heavy quarks with a hard mass of order T, are even easier, for then bare propagators and vertices can be used for the heavy quark. In either case, the proof of gauge invariance for the two-point $\mathscr{T}$-matrix elements goes through essentially unchanged. For instance, with a heavy quark [5], there is only the contribution similar to fig. 9a, with no diagram like fig. 9b. The difference between the contribution of fig. 9a in covariant and Coulomb gauges is given by eq. (4.49), except that the bare vertex γ^ν replaces $^*\Gamma^\nu$. This vanishes because the integral is odd in K.

We conclude this subsection by contrasting our calculations with those familiar at zero temperature [2]. As noted above, the effective Ward identities required at nonzero temperature have the same form as at zero temperature. Yet our manipulations appear rather more involved than the customary analysis. This is because what is usually established is merely unitarity – that only physical states contribute to the discontinuities of $\mathscr{T}$-matrix elements. For the two-point functions

we have shown a stronger statement, that the entire $\mathscr{S}$-matrix elements are gauge invariant. It is easier for us to show the latter, for in hot gauge theories unitarity is more complicated than at zero temperature. At zero temperature, unitarity means showing that the only contribution to the discontinuities of gauge invariant operators are from transverse modes. In a hot gauge theory, physical discontinuities receive contributions not just from the transverse modes, but over soft momenta, from the physical – but not the unphysical! – parts of the longitudinal modes.

4.3. BEYOND LEADING ORDER IN THE EFFECTIVE EXPANSION

In this subsection we discuss where corrections beyond leading order arise in the effective expansion. We consider the gluon self-energy as a typical example. In subsect. 4.2, we gave explicit expressions for some terms of order g in the gluon self-energy. Here we discuss where the remaining corrections of order g, and those of order g^2, arise.

Our discussion is schematic. The bare gluon propagator is written as Δ, the bare three- and four-gluon vertices as $g\Gamma_3$ and $g^2\Gamma_4$; the analogous effective quantities are ${}^*\Delta$, $g^*\Gamma_3$ and $g^2{}^*\Gamma_4$. We drop the color and space-time indices, as well as the momentum dependence of the vertices. Quarks are ignored, but could be incorporated in an obvious way. We label a loop correction as $O(g^n)$ if it is of order g^n relative to the corresponding tree amplitude.

To proceed systematically in the effective expansion, one starts with the bare action, $S_{\rm bare}$, and then adds and subtracts an action which generates all hard thermal loops, δS in eq. (3.35). In the effective expansion, amplitudes at "tree" level are generated by the sum, $S_{\rm bare} + \delta S$. The remainder, $-\delta S$, is treated perturbatively as a counterterm, to ensure that hard thermal loops are not double counted. Remember that the effective amplitudes generated by δS only enter when all momenta are soft; otherwise, bare quantities are used.

Before discussing corrections to the effective self-energy at soft momentum, we establish that the leading corrections to the self-energy at hard momentum are of $O(g^2)$, and that corrections to a vertex in which any leg is hard are at most of $O(g)$. For a gluon with hard momentum P, the leading corrections to the self-energy are

$$\Pi(P) = g^2\,\mathrm{Tr}_{(\mathrm{hard})}\,\Gamma_3\Delta(K)\Gamma_3\Delta(P-K) + g^2\,\mathrm{Tr}_{(\mathrm{hard})}\,\Gamma_4\Delta(K)$$
$$+ g^2\,\mathrm{Tr}_{(\mathrm{soft})}\,\Gamma_3{}^*\Delta(K)\Gamma_3\Delta(P-K)\,. \tag{4.50}$$

The integrals over hard k generate the usual terms at zero temperature, including the standard ultraviolet divergences, plus additional finite terms at nonzero temperature. The integral over soft k can be estimated by analogy to eq. (2.16). The

largest contribution occurs when each vertex Γ_3 is proportional to a hard momentum P. The statistical distribution function enters as $n(E_k) \simeq T/E_k$. If the external momentum P is near its mass-shell, some energy denominators are soft, $ip^0 - E_{p-k} \pm E_k \sim k$. The magnitude of the soft integral in eq. (4.50) is

$$g^2 \int_{\text{soft } k} \mathrm{d}^3k \frac{P^2}{E_{p-k}E_k} n(E_k) \frac{1}{ip^0 - E_{p-k} \pm E_k} \sim g^2 PT, \tag{4.51}$$

which is of $O(g^2)$ for $P \sim T$. Terms neglected in this estimate are down by more powers of g. In eq. (4.50), we did not include the soft integral involving the four-gluon vertex because it is of $O(g^3)$:

$$g^2 \operatorname{Tr}_{(\text{soft})} {}^*\Gamma_4^* \Delta(K) \sim g^2 \int_{\text{soft } k} \mathrm{d}^3k n(k) \frac{1}{k} \sim g^3 T^2. \tag{4.52}$$

If the gluon is not near its mass-shell, all energy denominators are hard, and the soft integral in eq. (4.50) is of $O(g^3)$; in this case the $O(g^2)$ corrections are given just by the hard integrals in eq. (4.50). The region near the mass-shell is often of the greatest interest, though: for example, the damping rate is determined by the discontinuity of the self-energy on mass-shell. For kinematic reasons the hard integral does not contribute to this discontinuity [4], and the damping rate is determined solely by the soft integral [5].

We remark that severe infrared divergences appear near the mass-shell, showing up in quantities such as wave function and vertex renormalization. At zero temperature these infrared divergences are logarithmic. At nonzero temperature, due to the behavior of the Bose–Einstein distribution function about zero energy, eq. (2.17), the mass-shell divergences become power-like: for massless particles, they are of the form $g^2T/(\omega - p)$ as $\omega \to p$. We assume that all such mass-shell divergences cancel in arbitrary discontinuities, and in physical quantities such as $\mathcal{S}$-matrix elements. In other words, for the purposes of power counting, we assume that a term such as $g^2T/(\omega - p)$ is of $O(g^2)$.

The corrections for a vertex in which any line is hard are similar to the hard self-energy of eq. (4.50). If all of the external momenta are hard, corrections from hard loops are of $O(g^2)$, with terms from soft loops down by more powers of g. For vertices in which the external lines are both hard and soft, the leading corrections can be of $O(g)$, as discussed following the power counting rules in sect. 2. Vertex corrections also exhibit mass-shell singularities; for instance, when two external momenta are equal, $P = Q$, they develop terms of the form $g^2T/(\omega - p)$.

With these results in hand, we consider the corrections to the gluon self-energy at soft momentum. Corrections of order g arise from diagrams at both one- and two-loop order.

(i) *One-loop diagrams.* We discuss separately the two cases in which the loop momenta are soft and hard.

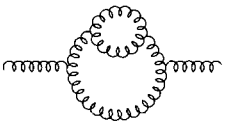

Fig. 10. A two-loop diagram which contributes to the gluon self-energy.

– Soft loop. These are the corrections $^*\Pi$ which are given in eq. (4.21).

– Hard loop. The hard-loop gives terms of O(1), which are cancelled by $\delta\Pi$ in the counterterm $-\delta S$. The hard loop, however, also includes subleading terms of O(g). For example, in going from eq. (2.16) to eq. (2.23) in sect. 2, we neglected terms that are p/k times the hard thermal loop.

(ii) *Two-loop diagrams.* There are corrections of O(g) from two loop diagrams in which both loop momenta are hard. Consider, for example, the diagram of fig. 10. Fig. 10 is obtained from the hard one-loop diagram of fig. 3a by adding a self-energy correction at hard K, $\Pi(K)$, and one extra propagator, $1/K^2$. From eq. (4.50), $\Pi(K) \sim g^2T^2$. As seen in sect. 2, if the extra propagator corresponds to Landau damping, it can produce terms which are of order $1/gT^2$. In all, $\Pi(K)$ times the extra $1/K^2$ is g times smaller than fig. 3a. Since fig. 3a is of O(1), then, fig. 10 includes terms of O(g). It is notable that while corrections to the hard line are down by g^2, their effects within loop diagrams are suppressed merely by g because of Landau damping.

The corrections of O(g) from hard diagrams, at either one- or two-loop order, do not contribute to the imaginary part of the two-gluon $\mathscr{S}$-matrix element. The reason is just kinematical. The one-loop diagrams, such as fig. 3a, can be cut just through two lines, which by assumption are hard. These cuts are either those of Landau damping, and so below the light cone, or far above. The two-loop diagrams, such as fig. 10, can be cut either through two or three virtual lines. As both loops are hard, cutting through two virtual lines gives the same kind of discontinuities as for the hard one-loop diagram. If three lines are cut, a typical discontinuity at nonzero temperature occurs if one particle is absorbed from the thermal distribution, and two emitted into it. The imaginary part for this cut has support for $\omega = E_{k_1} + E_{p-k_1-k_2} - E_{k_2}$, with k_1 and k_2 the two momenta for each loop. If both k_1 and k_2 are hard, this becomes $\omega \simeq k_1 + |\boldsymbol{k}_1 + \boldsymbol{k}_2| - k_2$. Now while it is possible for this ω to be soft, it only occurs if $\boldsymbol{k}_1 \simeq -\boldsymbol{k}_2$. Because this happens just in a small part of phase space, fig. 10 only contributes to the discontinuity through terms that are O(g^2), and not O(g). This holds for all hard two-loop diagrams, however the momenta are routed: simply put, it is not easy for the sum or difference of three hard momenta to equal a soft momenta.

In subsect. 4.2 we showed that to O(g), the $\mathscr{S}$-matrix elements formed from the effective one-loop diagrams at soft loop momenta, $^*\Pi$, themselves form a gauge invariant set. Thus the $\mathscr{S}$-matrix element formed from the remaining terms of

$O(g)$ – from the hard one and two loop diagrams – comprise a separate, gauge invariant set. Since these diagrams do not have an imaginary part to $O(g)$, they do not contribute to the damping rates at leading order; they do, however, give corrections of order g^3T^2 to m_g^2.

To show that the effective expansion can be used to higher order, we discuss where terms of $O(g^2)$ arise in the gluon self-energy at soft momenta. They arise from diagrams with one, two, and three loops.

(i) *One-loop diagrams.* There are contributions of $O(g)$ from one-loop diagrams with either soft or hard loop momentum; these diagrams also have subleading terms of $O(g^2)$. These terms of $O(g^2)$ include all of those at zero temperature, such as the ultraviolet divergent terms which produce wave function renormalization, as well as additional finite terms at nonzero temperature.

(ii) *Two-loop diagrams.* We divide this class of corrections of $O(g^2)$ into three subclasses, according to whether the loop momenta are soft or hard.

– *Both loops soft.* In these diagrams effective propagators and vertices must be used throughout. The vertices include both the effective forms of the bare vertices, as well as new effective vertices generated by hard thermal loops. For instance, from the effective four gluon interaction, one pair of virtual gluons can be tied together at one-loop order, as in fig. 8b. The effective six gluon interaction, with two pairs of gluons tied together, contributes at two-loop order.

– *One soft and one hard loop.* Suppose in fig. 10 that the outer loop has soft momenta, while the self-energy correction has hard loop momenta. There is a corresponding diagram in which a counterterm for a hard thermal loop, $-\delta\Pi$, is inserted on one line. While the terms of O(1) in the hard loop cancel those in $-\delta\Pi$, there remain corrections of $O(g)$. Since the one-loop graph with soft momenta is itself of $O(g)$, in total these terms are of $O(g^2)$.

– *Both loops hard.* Hard two-loop graphs produce terms of $O(g)$. Thus there are subleading terms in these graphs, which contribute at $O(g^2)$. There are also hard two-loop graphs which first contribute at $O(g^2)$: the graph with two distinct four gluon vertices is one example.

(iii) *Three-loop diagrams.* Three-loop graphs in which every loop momentum is hard will, by the power counting above, produce terms that are $O(g^2)$.

In all of this we repeatedly used the separation into soft and hard momenta. While this separation is awkward, we stress that it is necessary. As defined, hard thermal loops include all terms of O(1), and occur just when every external momentum is soft. By dividing the momenta into soft and hard, and using effective quantities exclusively over soft momenta, our resummation only includes terms of O(1).

Suppose that one did not divide the momenta into soft and hard, and attempted to use effective quantities even when the external momenta are hard. This would represent a further resummation of perturbation theory, in which terms that are strictly of $O(g)$ and higher are included. This further resummation appears to be

relatively innocuous, so long as the higher-order corrections included by this resummation are not double-counted.

With a further resummation, however, the cancellation of mass-shell singularities is not automatic. Mass-shell singularities only arise at hard momenta, since at soft momenta the effective mass-shells are well above the light cone. Typically, mass-shell singularities involve a propagator correction such as $1 + cg^2T/(\omega - p)$, cancelling against a vertex correction like $1 - cg^2T/(\omega - p)$. This cancellation fails if a further resummation is attempted. This is because the terms which produce mass-shell singularities are not the same as those which generate hard thermal loops. For example, in the propagator the terms which produce a hard thermal loop at soft momenta produce part, but not all of the mass-shell singularity at hard momenta: they contribute $c'g^2T/(\omega - p)$ to a propagator correction, with $c' \neq c$. In part, a further resummation consists of writing the corrections to the propagator as $[1 + (c - c')g^2T/(\omega - p)]/[1 - c'g^2T/(\omega - p)]$. The mass-shell divergences in this expression cancel against those of the vertex, but only when it is expanded out in g – in which case one is not performing a further resummation.

The problems with this further resummation are also illustrated in a recent work by Gatoff and Kapusta [3]. In this work they consider a partial resummation of terms of $O(g^2)$ at hard momenta. Doing so, they appear to find that their further resummation dramatically alters the analysis: loop corrections are $1/g$ times the corresponding terms at tree level, and completely overwhelm the usual hard thermal loop. This happens because when terms of $O(g^2)$ are retained in the hard self-energy, a small change in the mass-shell produces a large change in one over the energy denominators. Instead of this further resummation, we argue that perturbative corrections must always be treated as such. For the self-energy, instead of keeping terms of $O(g^2)$ in the energy denominators, they should be expanded out in powers of g. One can show that this avoids the pathologies found by Gatoff and Kapusta: at hard momenta neither mass-shells nor energy denominators change significantly, and consequently all corrections are of $O(g)$ or higher.

In the end, the best way to demonstrate the consistency of the effective expansion is to apply it to a wide variety of physical processes. Such calculations are in progress.

5. Conclusion

In this paper we laid out a general framework for studying soft processes in hot gauge theories. We showed how the hard thermal loop corrections can be resummed to all orders in the loop expansion into effective propagators and vertices, and that these can be used to generate a systematic expansion in g. We applied the effective expansion to the self-energy corrections for quarks and gluons at soft momenta, and showed that the two-point $\mathscr{T}$-matrix elements, on the effective

mass-shells, are gauge invariant. This solves the long-standing problem of the apparent gauge dependence in the gluon damping rate.

We stress that while our work was inspired by the problem of damping rates in hot QCD, the effective expansion is required for the calculation of *arbitrary* processes in *any* hot theory. It is needed in arbitrary processes, for while the effective expansion only differs from the bare expansion over soft momenta, inevitably soft momenta contribute to amplitudes at some finite order in g. The order at which this happens depends upon the process. Naive power counting suggests that the higher the mass dimension of the quantity under consideration, the higher the power in g at which effects of soft momenta first enter. Thus all of the complications which arise in the gluon damping rate at lowest order do not appear until higher order for other quantities of interest, such as the free energy. We intend to study these questions in future work.

Similarly, the effective expansion is necessary not just in hot QCD, but for all hot theories. One obvious example, in which the need for resummation does not seem to have been appreciated, is hot QED. Another example involves gauge theories coupled to scalars, such as for the phase transition at which the symmetry is restored in the weak interactions [8]. Since the transition temperature occurs at a temperature T_c of order $1/g$ times a zero temperature mass scale, our methods can be adapted to this example. The calculation of T_c in ref. [8] is given, in our language, by the hard thermal loops, and so to leading order is correct. To determine T_c beyond leading order, however, requires the full effective expansion, as modified to include the effects of symmetry breaking below T_c.

We conclude by noting that although the language and methods appear very different, there are close similarities between our analysis and transport theory. Indeed, originally Silin used kinetic theory to derive the hard thermal loop in the photon's self-energy [9]. The hard thermal loops in the quark and gluon self-energies can also be computed in this way [10]; surely this can be extended to our classification of arbitrary hard thermal loops in sects. 2 and 3. More significantly, in order to develop a complete and consistent transport theory, our program of an effective expansion over soft momenta – including both effective propagators and vertices – must be employed.

Note added

We have treated S-matrix elements at nonzero temperature in a manner very similar to that at zero temperature. Yet is is known that there are no stable asymptotic states at nonzero temperature, and hence no "true" scattering matrix [4, 17]. While this will not enter into our calculations until higher order, we suggest that the apparent difficulties this presents can be overcome. At nonzero temperature, define a S-matrix in the usual way, by evaluating each leg on the physical pole. Since each pole is (eventually) off the physical sheet, this is not a true

scattering matrix. Yet we suggest that this S-matrix *is* a gauge invariant quantity, containing physical information about the approach to equilibrium. This view is encouraged by recent work from Kobes et al. [18]. They elegantly show, in a manner directly applicable to nonzero temperature, that the poles of physical transverse and longitudinal gluons have a gauge invariant position. This is a necessary condition for arbitrary S-matrix elements, as defined above, to be gauge invariant.

After we submitted this work for publication, we received a preprint by Frenkel and Taylor [19]. They study the hard thermal loops in the N-gluon amplitudes, deriving some of the identities given in sect. 2. They observe that hard thermal loops obey the simple Ward identities of eqs. (2.40) and (2.41). They also derive some new identities that allow the hard thermal loop in the four-gluon amplitude to be written in a simpler form than eq. (3.28): it is proportional to $N_c + N_f/2$. Although they did not discuss amplitudes with external quarks, similar identities can be used to show that the hard thermal loop in the amplitude between a quark pair and two gluons, eq. (3.29), is proportional to C_f. Frenkel and Taylor find that the hard thermal loops in the N-gluon amplitudes are equal in axial and Feynman gauges; this is similar to our demonstration, in subsects. 3.1 and 3.2, of their equality in Coulomb and Feynman gauges. They do not prove that these loops are the same in arbitrary covariant gauges, which we established in subsect. 3.3.

Lastly, T. Evans and R. Kobes pointed out that the result discussed at the end of appendix A – that at one-loop order, only single powers of the statistical distribution functions enter – can be easily proven. Evaluate the sum over k^0 in standard fashion, using a contour integral over complex k^0 of the integrand times $\cot(k^0/2T)$ (or $\tan(k^0/2T)$). Then no matter how many poles there are, since only one power of cot or tan enters, at most single factors of $n(E)$ (or $\tilde{n}(E)$) ever appear to one-loop order.

Appendix A

ONE-LOOP INTEGRALS AND CUTTING RULES

In this appendix we reduce the integrals which arise at one-loop order in the two-, three- and four-point functions to integrals over the three-momentum $\boldsymbol{k}$. These examples illustrate general features, discussed in sect. 2, which allow us to isolate the hard thermal loops in arbitrary N-point functions. These integrals also represent all of those needed for the explicit calculation of the damping rates [14].

To treat boson and fermion propagators in a unified way, we introduce an index "r", $r = +$ for bosons and $r = -$ for fermions:

$$\Delta(K) \equiv \Delta^{+}(K), \qquad \tilde{\Delta}(K) \equiv \Delta^{-}(K). \tag{A.1}$$

All momenta are assumed to be euclidean, so the index r_K for a momentum K is $r_K = e^{ik^0/T}$. Indices are multiplicative: for a propagator $\Delta^r(P-K)$, $r = r_P r_K$. We use the index r to distinguish between Bose–Einstein and Fermi–Dirac statistics:

$$n^+(E) = n(E), \qquad n^-(E) = \tilde{n}(E). \tag{A.2}$$

Finally, we introduce the statistical distribution functions $f_s^r(E)$, where $s = +$ denotes emission, and $s = -$ denotes absorption:

$$f_+^r(E) = 1 + rn^r(E), \qquad f_-^r(E) = rn^r(E). \tag{A.3}$$

The distribution functions satisfy the simple identities

$$f_{-s}^r(E) = r\,e^{-sE/T} f_s^r(E), \tag{A.4}$$

$$f_s^r(E) - f_{-s}^r(E) = s. \tag{A.5}$$

They also satisfy

$$f_s^r(E) f_{s'}^{r'}(E') - f_{-s}^r(E) f_{-s'}^{r'}(E') = \frac{s+s'}{2} + s'rn^r(E) + sr'n^{r'}(E'). \tag{A.6}$$

Note that the terms quadratic in the statistical distribution functions cancel.

The boson and fermion propagators of eqs. (2.4) and (2.8) can be written as

$$\Delta^r(\tau, E) = \frac{1}{2E} \sum_{s=\pm} f_s^r(E) e^{-sE\tau}, \qquad 0 \leqslant \tau \leqslant \frac{1}{T}, \tag{A.7}$$

where $E \equiv k$. For purposes of calculation, it is essential to remember that this representation is valid *only* for $0 \leqslant \tau \leqslant 1/T$. If an integral depends upon a value of τ outside of this range, the propagator must be transformed so that τ lies within this range. This is done by using the periodicity condition

$$\Delta^r(\tau + m/T, E) = r^m \Delta^r(\tau, E). \tag{A.8}$$

In this appendix we consider for simplicity traces with no powers of K^μ in the numerator. Integrals involving powers of K^μ can be easily found from these results. Powers of the spatial momentum k^i just tag along, while single powers of k^0 can be replaced by derivatives with respect to τ, which give $\pm iE$. Integrals involving higher powers of k^0 can be reduced to at most single powers of k^0 by using $(k^0)^2 = K^2 - k^2$ repeatedly.

We introduce some further notation to simplify our formulae. For integrals which involve the propagator $\Delta^{r_l}(P_l - K)$, define $E_l = |\boldsymbol{p}_l - \boldsymbol{k}|$; Fourier transformation then produces $\Delta^{r_l}(\tau_l, E_l)$, which can be expressed in terms of $f_{s_l}^{r_l}$ using

eq. (A.7). In the distribution functions the explicit dependence on E_l is dropped: $f_{s_l}^{r_l} \equiv f_{s_l}^{r_l}(E_l)$. For a trace with j propagators, the integration element over the three-momentum $\boldsymbol{k}$, times the residues of all the propagators, is defined to be $\mathscr{D}_j k$:

$$\int \mathscr{D}_j k \equiv \int \frac{\mathrm{d}^3 k}{(2\pi)^3} \prod_{l=0}^{j-1} \frac{1}{2E_l} . \tag{A.9}$$

We start with an integral which arises in the two-point functions:

$$\mathscr{I}_2 = \mathrm{Tr}\, \Delta^r(K)\, \Delta^{r_1}(P_1 - K) . \tag{A.10}$$

Eq. (2.5) is used to introduce $\Delta^r(\tau, E)$ and $\Delta^{r_1}(\tau_1, E_1)$. The sum over k^0 gives a delta-function which sets $\tau_1 = \tau$, with a result like eq. (2.15). Note that in this case there is no problem with the region of integration. With eq. (A.7) the τ integral is elementary:

$$\mathscr{I}_2 = \int \mathscr{D}_2 k \sum_{s, s_1 = \pm} \frac{-1}{ip_1^0 - sE - s_1 E_1} \left(f_s^r f_{s_1}^{r_1} - f_{-s}^r f_{-s_1}^{r_1} \right), \tag{A.11}$$

where we have also used eq. (A.4). Although two powers of the f_s^r's enter in eq. (A.11), because of eq. (A.6), no more than single powers of $n(E)$ or $\tilde{n}(E)$ occur: term by term, double powers of the distribution functions cancel between emission and absorption.

The trace with three propagators illustrates the complications which arise when there is more than one τ integral:

$$\mathscr{I}_3 = \mathrm{Tr}\, \Delta^r(K)\, \Delta^{r_1}(P_1 - K)\, \Delta^{r_2}(P_2 - K) . \tag{A.12}$$

Introducing τ integrals for each propagator, and doing the sum over k^0 to eliminate the τ_2 integral,

$$\mathscr{I}_3 = \int \frac{\mathrm{d}^3 k}{(2\pi)^3} \int_0^{1/T} \mathrm{d}\tau \int_0^{1/T} \mathrm{d}\tau_1\, \mathrm{e}^{i(p_1^0 \tau_1 + p_2^0 (\tau - \tau_1))} \Delta^r(\tau, E)\, \Delta^{r_1}(\tau_1, E_1)\, \Delta^{r_2}(\tau - \tau_1, E_2) . \tag{A.13}$$

In $\Delta^{r_2}(\tau - \tau_1, E_2)$, the regions $\tau > \tau_1$ and $\tau < \tau_1$ must be treated separately:

$$\Delta^{r_2}(\tau - \tau_1, E_2) = \theta(\tau - \tau_1)\, \Delta^{r_2}(\tau - \tau_1, E_2) + \theta(-\tau + \tau_1) r_2\, \Delta^{r_2}(\tau - \tau_1 + 1/T, E_2) , \tag{A.14}$$

where $\theta(x)$ is the step function: $\theta(x) = +1$ for $x > 0$, $\theta(x) = 0$ for $x < 0$. In eq. (A.14) we have used eq. (A.8) to ensure that for both terms the argument in τ lies between 0 and $1/T$, so that the representation of eq. (A.7) can be employed. From eq. (A.4),

$$\Delta^{r_2}(\tau - \tau_1, E_2) = \frac{1}{2E_2} \sum_{s_2 = \pm} e^{-s_2 E_2(\tau - \tau_1)} \left(\theta(\tau - \tau_1) f_{s_2}^{r_2} + \theta(-\tau + \tau_1) f_{-s_2}^{r_2} \right). \quad \text{(A.15)}$$

Doing the τ integral,

$$\mathcal{I}_3 = \int \mathcal{D}_3 k \int_0^{1/T} d\tau \sum_{s, s_1, s_2 = \pm} f_s^r \, e^{(ip_2^0 - sE - s_2 E_2)\tau}$$

$$\times \frac{1}{i(p_1^0 - p_2^0) - s_1 E_1 + s_2 E_2} \left(-s_1 f_{s_2}^{r_2} + s_2 f_{s_1}^{r_1} \, e^{(i(p_1^0 - p_2^0) - s_1 E_1 + s_2 E_2)\tau} \right). \quad \text{(A.16)}$$

The terms from $\tau > \tau_1$ and $\tau < \tau_1$ have been combined, and eq. (A.5) used to simplify the expression. After doing the τ integral, eq. (A.16) reduces to a sum of integrals similar to $\mathcal{I}_2$,

$$\mathcal{I}_3 = \int \mathcal{D}_3 k \sum_{s, s_1, s_2 = \pm} \frac{1}{i(p_1^0 - p_2^0) - s_1 E_1 + s_2 E_2}$$

$$\times \left(\frac{s_1}{ip_2^0 - sE - s_2 E_2} \left(f_s^r f_{s_2}^{r_2} - f_{-s}^r f_{-s_2}^{r_2} \right) - \frac{s_2}{ip_1^0 - sE - s_1 E_1} \left(f_s^r f_{s_1}^{r_1} - f_{-s}^r f_{-s_1}^{r_1} \right) \right). \quad \text{(A.17)}$$

Note that by eq. (A.6), at most single powers of $n(E)$ and $\bar{n}(E)$ survive. This cancellation of higher powers of the distribution functions is only evident because we performed the integrals in the order we did, integrating first over τ_1, collecting all terms, and then doing the τ integral.

Another way of calculating eq. (A.13) would be to follow Baym and Sessler, and Dzyaloshinski [13], who originally developed this "noncovariant" approach. These authors always do the integral over the smallest time first. Thus for $\tau > \tau_1$, they integrate over τ_1 and then over τ (as we do), but for $\tau < \tau_1$, they integrate in the reverse order, over τ and then τ_1. As discussed in sect. III of Baym and Sessler [13], this has some advantages, in that series of terms can be systematically regrouped. With their technique, though, the cancellation of higher powers of the $n(E)$'s in one-loop diagrams is only apparent after all terms had been regrouped over common energy denominators. By keeping uniformly to the same order of

integration in the τ's, we make these cancellations manifest as each succeeding τ integral is done.

The trace that arises in the four-point functions is

$$\mathscr{I}_4 = \mathrm{Tr}\,\Delta^r(K)\Delta^{r_1}(P_1-K)\Delta^{r_2}(P_2-K)\Delta^{r_3}(P_3-K)\,. \tag{A.18}$$

We perform this integral as follows. Times τ, τ_1, τ_2, τ_3 are introduced for each propagator. Using the sum over k^0 to eliminate $\tau_3 = \tau - \tau_1 - \tau_2$, we integrate over τ_2, then τ_1, and finally over τ. The result is

$$\begin{aligned}\mathscr{I}_4 = \int \mathscr{D}_4 k \sum_{s,s_1,s_2,s_3=\pm} & \frac{1}{i(p_2^0-p_3^0)-s_2E_2+s_3E_3} \\ \times\Bigg[& \frac{s_2}{i(p_1^0-p_3^0)-s_1E_1+s_3E_3}\left(\frac{s_3}{ip_1^0-sE-s_1E_1}\left(f_s^r f_{s_1}^{r_1}-f_{-s}^r f_{-s_1}^{r_1}\right)\right. \\ & \left. -\frac{s_1}{ip_3^0-sE-s_3E_3}\left(f_s^r f_{s_3}^{r_3}-f_{-s}^r f_{-s_3}^{r_3}\right)\right) \\ & +\frac{s_3}{i(p_1^0-p_2^0)-s_1E_1+s_2E_2}\left(\frac{s_1}{ip_2^0-sE-s_2E_2}\left(f_s^r f_{s_2}^{r_2}-f_{-s}^r f_{-s_2}^{r_2}\right)\right. \\ & \left.\left. -\frac{s_2}{ip_1^0-sE-s_1E_1}\left(f_s^r f_{s_1}^{r_1}-f_{-s}^r f_{-s_1}^{r_1}\right)\right)\right]. \end{aligned} \tag{A.19}$$

From eq. (A.6) it is apparent that only single powers of the distribution functions survive.

We now discuss a remarkable feature that is crucial to our power counting estimates for hard thermal loops in sect. 2. We assert that for arbitrary N-point functions at one-loop order, there are never more than single powers of the statistical distribution functions. Originally, each of the N noncovariant propagators brings in a factor of $n(E)$ or $\tilde{n}(E)$, but after all the τ integrals are done, all multiple powers of $n(E)$ and $\tilde{n}(E)$ cancel. This is demonstrated explicitly by our results for the two-, three-, and four-point functions. These cancellations are a consequence of how the cutting rules work at nonzero temperature. The discontinuity in a one-loop diagram is a sum of cuts through two virtual lines: the cut lines are put on their mass-shell, and the rest of the diagram is the product of two disjoint tree amplitudes. This is familiar at zero temperature. Computing the diagram at $T=0$ noncovariantly, we get a sum over products of energy denominators, as in eqs. (2.16), except that in factors such as $1+n(E)$, only the 1 is kept. A discontinuity is produced by the analytic continuation of an external euclidean energy p^0 to $-i(\omega+i\epsilon)$. This turns one energy denominator, involving p^0, into a delta-function in ω. The energy denominators which are not cut, combine to give

the two disjoint tree amplitudes, by identities such as

$$\frac{1}{ip^0+p}-\frac{1}{ip^0-p}=2p\frac{1}{P^2}\,. \tag{A.20}$$

The factors of $2p$ on the r.h.s. cancel the residues, $1/2p$, in the noncovariant propagators.

At nonzero temperature the cutting rules go through in much the same way [4, 16]. Isolate the part of the discontinuity which arises from cutting through two gluon lines in a diagram. There must be factors of $n(E)$ for the two cut lines, since each cut line is either emitted into or absorbed from the thermal distribution, with probabilities $1+n(E)$ or $n(E)$, respectively. The double powers of $n(E)$ associated with the two cut lines, cancel between emission and absorption as in eq. (A.6). For a given cutting, however, the factors of $n(E)$ or $\bar{n}(E)$ associated with the uncut lines must cancel. If they did not, the identities analogous to eq. (A.20) would not go through, and the uncut energy denominators would not reduce to a product of disjoint tree amplitudes.

It is easy to conjecture how this result generalizes to higher loop order. We suggest that for arbitrary N-point amplitudes computed to L-loop order, the integral can always be written in a form in which at most L factors of the statistical distribution functions appear.

References

[1] J. Cleymans, R.V. Gavai and E. Suhonen, Phys. Rep. 130 (1986) 217;
L. McLerran, Rev. Mod. Phys. 58 (1986) 1021;
B. Svetitsky, Phys. Rep. 132 (1986) 1;
N.P. Landsman and Ch.G. van Weert, Phys. Rep. 145 (1987) 141

[2] G. 't Hooft, Nucl. Phys. B33 (1971) 173;
G. 't Hooft and M. Veltman, Nucl. Phys. B50 (1972) 318;
B.W. Lee and J. Zinn-Justin, Phys. Rev. D5 (1972) 3121, 3137

[3] O.K. Kalashnikov and V.V. Klimov, Sov. J. Nucl. Phys. 31 (1980) 699;
D.J. Gross, R.D. Pisarski and L.G. Yaffe, Rev. Mod. Phys. 53 (1981) 43;
K. Kajantie and J. Kapusta, Ann. Phys. (N.Y.) 160 (1985) 477;
J.A. Lopez, J.C. Parikh, and P.J. Siemens, Texas A&M report, 1985 (unpublished);
T.H. Hansson and I. Zahed, Phys. Rev. Lett. 58 (1987) 2397; Nucl. Phys. B292 (1987) 725;
U. Heinz, K. Kajantie and T. Toimela, Phys. Lett. B183 (1987) 96; Ann. Phys. (N.Y.) 176 (1987) 218;
H.-Th. Elze, U. Heinz, K. Kajantie and T. Toimela, Z. Phys. C37 (1988) 305;
H.-Th. Elze, K. Kajantie and T. Toimela, Z. Phys. C37 (1988) 601;
R. Kobes and G. Kunstatter, Phys. Rev. Lett. 61 (1988) 392;
S. Nadkarni, Phys. Rev. Lett. 61 (1988) 396;
J.C. Parikh and P.J. Siemens, Phys. Rev. D37 (1988) 3246;
H.-Th. Elze, CERN preprint CERN-TH.5223/88 (1988);
M.E. Carrington, T.H. Hansson, H. Yamagishi and I. Zahed, Ann. Phys. (N.Y.) 190 (1989) 373;
M.E. Carrington, H. Yamagishi and I. Zahed, Stonybrook preprint 88-0556 (1988);
J. Milana, Phys. Rev. D39 (1989) 2419;
G. Gatoff and J. Kapusta, Phys. Rev. D41 (1990) 611;

J. Kapusta and T. Toimela, Phys. Rev. D39 (1989) 3197;
R. Kobes, G. Kunstatter and K.W. Mak, Phys. Lett. B223 (1989) 433;
J.C. Parikh, P.J. Siemens and J.A. Lopez, Pramana–J. Phys. 32 (1989) 555;
U. Kraemmer, M. Kreuzer and A. Rebhan, Hannover preprint ITP-UH 8/89;
M. Kreuzer, A. Rebhan and H. Schulz, Santa Barbara preprint NSF-ITP-89-203;
U. Kraemmer, M. Kreuzer, A. Rebhan and H. Schulz, to appear in *Lecture Notes in Physics*, Proc. of the "Workshop on Physical and Non-Standard Gauges", Vienna, Austria, 1989;
V.V. Lebedev and A.V. Smilga, Bern preprint BUTP-89/25

[4] R.D. Pisarski, Nucl. Phys. B309 (1988) 476

[5] R.D. Pisarski, Physica A158 (1989) 246; Phys. Rev. Lett. 63 (1989) 1129

[6] E. Braaten and R.D. Pisarski, Northwestern preprint NUHEP-TH-89-12, to appear in Phys. Rev. Lett.

[7] M. Gell-Mann and K.A. Brueckner, Phys. Rev. 106 (1957) 364

[8] D.A. Kirzhnits and A.D. Linde, Phys. Lett. B42 (1972) 472;
S. Weinberg, Phys. Rev. D9 (1974) 3357;
L. Dolan and R. Jackiw, Phys. Rev. D9 (1974) 3320;
Y. Ueda, Phys. Rev. D23 (1981) 1383

[9] V.P. Silin, Sov. Phys. JETP 11 (1960) 1136

[10] Physical Kinetics, E.M. Lifschitz and L.P. Pitaevski (Pergamon Press, London, 1981), pp. 132–136;
V.P. Silin and V.N. Ursov, Lebedev Institute Reports (Sov. Phys.) 1 (1982) 34; 12 (1982) 53; 1 (1986) 40; 5 (1988) 33;
U. Heinz and P.J. Siemens, Phys. Lett. B158 (1985) 11;
U. Heinz, Ann. Phys. (N.Y.) 168 (1986) 148;
D.G. Lominadze, G.I. Melikidze, V.P. Silin and V.N. Ursov, Sov. J. Plasma Phys. 12 (1986) 468;
H.-Th. Elze, M. Gyulassy and D. Vasak, Phys. Lett. B177 (1986) 402, Nucl. Phys. B276 (1986) 706;
H.-Th. Elze, Z. Phys. C38 (1988) 211;
M.-C. Chu and T. Matsui, Phys. Rev. D39 (1989) 1892;
G. Baym, H. Monien and C.J. Pethick, Proc. 16th Int. Workshop on Gross properties of nuclei and nuclear excitations, Hirschegg, Austria, ed. H. Beldmeier (GSI and Institut fur Kernfysik, Darmstadt, 1988), 128;
C.J. Pethick, G. Baym and H. Monien, Nucl. Phys. A498 (1989) 313c;
G. Baym, H. Monien, C.J. Pethick and D.G. Ravenhall, Univ. of Illinois preprint, Jan. 1990;
S. Mrowczynski, Acta Phys. Pol. B19 (1988) 91; to appear in Quark-Gluon Plasma, ed. by R. Hwa (World Scientific); Phys. Rev. D39 (1989) 1940; Physica A158 (1989) 136 and 225;
H.-Th. Elze and U. Heinz, Phys. Rep. 183 (1989) 81;
H.-Th. Elze, CERN preprint CERN-TH.5423/89, CERN-TH.5574/89

[11] O.K. Kalashnikov and V.V. Klimov, ref. [3];
V.V. Klimov, Sov. J. Nucl. Phys. 33 (1981) 934; Sov. Phys. JETP 55 (1982) 199;
H.A. Weldon, Phys. Rev. D26 (1982) 1394, 2789; unpublished, presented at the Univ. of Minnesota, Oct. 1987; Physica A158 (1989) 169; Phys. Rev. D40 (1989) 2410

[12] R.D. Pisarski, Nucl. Phys. A498 (1989) 423c; Physica A158 (1989) 146; Fermilab preprint 88/113-T (unpublished)

[13] R. Balian and C. De Dominicus, Nucl. Phys. 16 (1960) 502;
G. Baym and A.M. Sessler, Phys. Rev. 131 (1963) 2345;
I.E. Dzyaloshinski, Sov. Phys. JETP 15 (1962) 778

[14] E. Braaten and R.D. Pisarski, Brookhaven preprint BNL-43882;
E. Braaten, R.D. Pisarski, and T.C. Yuan, Brookhaven preprint BNL-43941, and work in progress

[15] C. Itzykson and J.-B. Zuber, Quantum Field Theory (McGraw-Hill, New York, 1980), p. 87

[16] L.P. Kadanoff and G. Baym, Quantum statistical mechanics (Benjamin, Reading, 1978);
H.A. Weldon, Phys. Rev. D28 (1983) 2007

[17] H. Narnhofer, M. Requardt and W. Thirring, Commun. Math. Phys. 92 (1983) 247;
N.P. Landsman, Ann. Phys. (N.Y.) 186 (1988) 141

[18] R. Kobes, R. Kunstatter and A. Rebhan, Univ. of Winnipeg preprint, Oct. 1989

[19] J. Frenkel and J.C. Taylor, Cambridge Univ. preprint, DAMTP-89-23